Preface

The Master Thesis enacts as the final step in completing the Master of Science degree at the Mechanical Engineering program at the Faculty of Engineering, Lund University, Sweden. The thesis was completed at the Department of Design Sciences with the cooperation of ASSA ABLOY Entrance Systems.

We would like to thank our supervisor Per-Erik Andersson, Division of Machine Design, Department of Design Sciences, LTH. Also, thanks to supervisors at ASSA ABLOY Entrance Systems Sven Åsbo, Design Manager and Ann-Sofie Engström, Design Engineer. We send our gratitude to Lars Vedmar, Division of Machine Element and Srinivasan Iyengar, Division of Materials Engineering for their support and patience when answering our questions. Thanks to Leif Tordelius, ASSA ABLOY Entrance Systems and Lennart Strömberg, Department of Design Sciences for helping us with the design of the prototype.

Lastly, we would like to thank our families, Angela Huang and Marie Feldt for their support during our study.

August 31st 2009, Lund, Sweden

Karl-Oskar Finnman and Tobias Persson

Abstract

Title: Lifetime Prediction for Wheel/Track Contact - Creation of a Practical and Theoretical Model

Authors: Karl-Oskar Finnman, Tobias Persson, *Department of Design Sciences*

Supervisors: Per-Erik Andersson, *Department of Design Sciences, at the Faculty of Engineering, Lund University*

Ann-Sofie Engström, *Design Engineer, ASSA ABLOY Entrance Systems.*

Objective: To limit the research time by developing a theoretical model, that can predict the lifetime of a wheel with the help of different input values. Apart from a theoretical model, also create a different type of test rig that can decrease the testing time, and still produce an accurate result similar to a real situation.

Method: This Master's Thesis was based on both an investigatory method and a product development method.

Conclusions: With the mathematical model created in the study, it is possible to predict lifetime of a wheel/track combination by imputing data from a short time test with high contact force. Then it will be able to predict how long a test using normal contact forces will last. In addition, it will be possible to optimize the wheel/track to make them smaller if a specific pressure is given.

The prototype of the new test rig displays that it is possible to design a lightweight testing rig with the possibility to increase the speed of a wheel/track lifetime testing. The new test rig uses the same carriage wheel and sliding track as present test rig. Moreover, all its components are made with an easy conversion in mind and at minimal cost.

Keywords: Hertzian pressure, sliding door, test rig, wear, wheel/track contact

Sammanfattning

Dagens testmetoder för skjutdörrar tar väldigt lång tid att genomföra då man oftast använder normala förhållanden så som öppnings- och stängningshastighet. Detta leder till att när en ny konfiguration tas fram så tar det lång tid innan den kan lanseras. Sätt att förkorta testningen är då att föredra när tidskrävande test normalt är kostsamma vilket är bakgrunden till att denna studie genomfördes.

Studien är uppdelad i två delar, en teoretisk och en praktisk.

Som förstudie till den teoretiska modellen studerades olika typer av förslitningar för att se vilka som inverkar vid en hjul/glidbana konfiguration. Förslitningar så som Adhesiv nötning, Abrasiv nötning och utmattningsförslitning undersöktes. Även kontakten i sig studerades i form av hertz kontaktteori.

I den teoretiska delen användes ljusmikroskop för att kontrollera om det blev någon förslitning på hjul och bana detta för att verifiera vilken förslitning som är den dominerande. Förslitningen visade sig i huvudsak vara minimal på de undersökta hjulen och glidbanorna vilket ledde till att ekvationen för slitagevolymen ej kunde verifieras. Istället användes sambandet av förhållandet mellan kraft och antalet rotationer till att förutse ett längre test. Då förslitningen var minimal på den befintliga konstruktionen togs det även fram bättre hjul/glidbane kombinationer med hjälp av kontaktteorin för användning på lättare skjutdörrar. Kontaktteorin i sig verifierades med FEM-analys vilket gav i princip samma resultat.

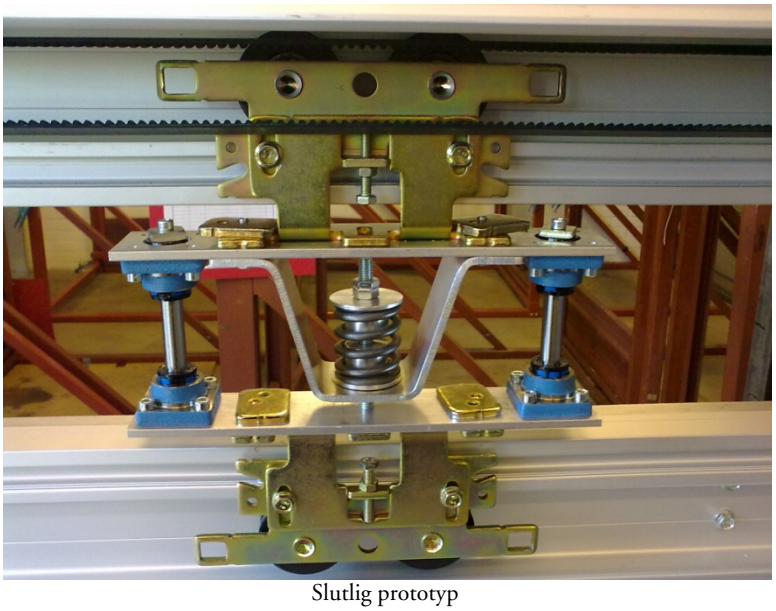

Slutlig prototyp

I den praktiska delen togs en testrigg fram för att förbättra och påskynda testningen av hjul och glidbana. Därefter delades problemet upp i två delproblem (krafttyp och bantyp) där principlösningar togs fram inom varje. En utvärdering av dessa gjordes mot den befintliga testmetoden för att få fram ett vinnande förslag från varje delproblem. Sedan kombinerades de ihop med varandra för att skapa det slutliga lösningsförslaget som består av en fjäder som kraftöverföring och två befintliga bärprofiler som bana där en av bärprofilerna placeras upp och ner. För att kombinera de två delproblemen med varandra konstruerades en sammandragande konstruktion som en vidareutveckling som analyserades.

Därefter skapades en prototyp utifrån det slutliga lösningsförslaget som byggdes samman vid ASSA ABLOY Entrance Systems i Landskrona. På plats löstes problem som uppstod där ett var att glidbanan lämnade sitt läge på den undre aluminiumprofilen vilket löstes med skruvar. Prototypen testkördes med en medellast vilket den klarade utan problem. Resultatet från körningen visade att det är möjligt att testa hjul/glidbana på ett tillfredställande sätt utan dörr med en mindre massa som i sin tur kan köras snabbare och korta hjul/glidbane testningen.

Slutsatserna från studien blev att det är möjligt att förkorta test tiden genom matematiska samband mellan kraft och rotationer samt ett nytt sätt att genomföra testning utan att använda en dörr.

Table of Contents

1. Introduction

1.1 Background

Today the testing of sliding doors is a very time-consuming matter, therefore a more efficient way have to be developed. For example, a normal test rig currently used in the industry takes approximately six[1] months to verify if a new wheel type is good enough for its purpose. This kind of testing works in the way that the door will open and close in normal conditions with a regular velocity. Although this system is slow, it is still all right because it gives an accurate result. However, the creation of a new type of testing system is important because time-consuming tests are expensive.

The main parts of the sliding door of most concern are the wheel and track, and with the study, a better knowledge of their lifetime is of interest. The weaker of these two, usually the one with the least toughness will be of most interest to study. Both the wheel and track pay an important role for the sliding door, they are the main element deciding; how smooth the door will open and the lifetime of the door. That is why this study covers those two components.

Figure 1. Sliding door

[1] Sven Åsbo, Design Manager, ASSA ABLOY Entrance System

1.2 Related Work

No much information that are specifically about sliding doors or similar were found. The related work found during the literature study was mainly of railroads and train wheels. This area is very important because of the safety required during the transportation of people. Therefore, extensive studies of train wheels exist with different types of equations and simulations to predict its performance. Although there are big differences when comparing with a sliding door, some similarities do exist for instance contact equations and temperature rise, which are of used for the study.

Figure 2. Railway wheel on rail

1.3 The Company

Most parts of the material used for this study was provided by ASSA ABLOY Entrance System since the study is a joint effort with the company. ASSA ABLOY Entrance System is a branch of ASSA ABLOY. They produce, sell and offer service for a complete line of automatic door systems for the global market. The unit created in 2002 when ASSA ABLOY took over ownership of Besam, although the name change they still sell their products under the trademark Besam. They have sales and direct service over the whole world and produce their products in China, Czech Republic, Sweden, United Kingdom and the United States of America. The branch has 2300 employees and the headquarters are located in Landskrona, Sweden (ASSA ABLOY, 2009).

1.4 Report Structure

A brief description of the different chapters in the study:

- **Chapter 1 – Introduction:**
  The chapter introduces the study, contains information about the main problems in the area and similar studies. Moreover, a brief statement about the assisting company.
- **Chapter 2 – Project Description:**
  The chapter contains a description of the objectives, the verification process and the project plan.
- **Chapter 3 – Theory:**
  Information about different wear types is available in this chapter, also definitions of the Hertz theory and stresses.
- **Chapter 4 – Theoretical Model:**
  This chapter describes the methods and results of the theoretical model.
- **Chapter 5 – Practical Device:**
  The development process of the test rig from idea to final product, all the steps taken on the way are available in this chapter.
- **Chapter 6 – Conclusions:**
  The chapter contains a brief restatement of the study aims and a summarization of the findings.

2. Project Description

2.1 Purpose

Verifying a wheel's property regarding its stress and wear resistance is very important during the work with developing new wheel types for sliding doors. The standard test today has the wheels assembled to a sliding door and driven for one million cycles[2], which can take up to six months to complete. In the developing process this step is very awkward, this because it leads to an increase in developing time and it will take a very long time to verify prototypes.

To limit the developing time there is an interest in developing a theoretical model, which could predict the lifetime of a wheel with the help of different input values. Apart from a theoretical model, also creation of a different type of test rig could decrease the testing time, and still produce an accurate result similar to a real situation.

2.1.1 Objectives for Theoretical Model

The purpose for this model is that it will be able to predict the lifetime of a wheel during pre-set conditions. Some of the input data that could be in the model are the following:

- Material of wheel and track.
- Temperature generation of wheel and track.
- The force applied on the wheel.
- The wheel's geometry.
- The speed of the wheel.
- Temperature surrounding the wheel.
- Different material layers of the wheel.
- Other aspects that might have an impact on the wheel.

First of all a clear definition of wear is essential, and apart from pure visual influence there should be consideration of changes in both dimensions and sound level.

[2] One cycle is when the door open and then close.

2.1.2 Objectives for Practical Device

The practical device should be able to test the lifetime of the wheel during similar conditions as a sliding door, but with a shorter time span. There have to be a possibility to test several wheels together that could have a different dimension and shape from each other. An option to change the force to up to 1000 N per wheel must be present. In addition, the track that the wheels follow should be changeable, making it easier to have different profiles for different types of wheels. Apart from that there have to be a function to control the speed and direction. A possibility to measure the travelled distance of the wheel should also exist.

2.1.3 Verification

Both the theoretical model and the practical device need verification with values from normal conditions of a sliding door. If possible a statistical model that connects the theoretical results and results from the reality should be made. Information about what kind of error rate that is acceptable could then be made with the help of ASSA ABLOY Entrance Systems' quality department.

2.2 Limitations

The study contains some limitations, because creating both a theoretical model and a practical device is a big task with many details to cover. Of the two, the practical model is of the most importance and should therefore have main priority. Only one type of wear was further studied (fatigue wear) because of the result from the microscopic analysis. In the theoretical model the aspect of surrounding temperature and different material layer were not covered. In the optimization part lifetime of bearing and size were excluded. For benchmarking only one type of test rig was reference, ASSA ABLOY Entrance Systems own testing system. The analysis done for the test rig was limited to static analysis. After the prototype was created and tested no time to do a statistical model was available because of time constraints.

2.3 Project Plan

It is important to have a plan set up before starting the research. A well structured project plan will provide a lifeline to follow, help during stalled progress and make the study more organized.

2.3.1 Gantt chart

A Gantt chart is a good example for keeping track of the workload required, and the one used for this study is illustrated in Figure 3.

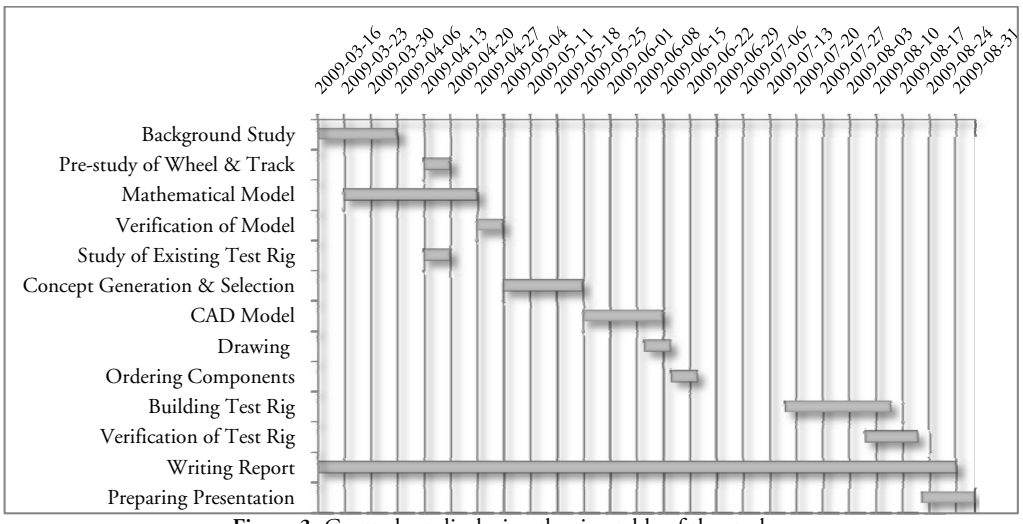

Figure 3. Gantt chart displaying the timetable of the study.

2.3.2 Project Steps

A brief description of the different phases in the study taken from the Gantt chart:

- **Background study:**
  A literature study of the subject and visit the company to get a better understanding of the problem at hand.

- **Study of wheel, track and test rig:**
  Plan for another visit to ASSA Entrance Systems to study the existing test rig and learn more about the problem.

- **Mathematical Model:**
  Creation of a mathematical model that will help in determining if a wheel or track will function properly before it is tested.

- **Verification of Model:**
  Making a verification of the model with the help of a real test or similar to see if the mathematical result is valid or not.

- **Concept Generation and Selection:**
  Coming up with ideas of a new test rig and evaluating the ideas using the Ulrich and Eppinger method (Ulrich & Eppinger, 2008).

- **CAD model:**
  After selecting a winning concept, the next step will be to develop a working prototype using a CAD environment.

- **Drawing:**
  Once the CAD models are finished, they need to be converted into blueprints that are used for creating or ordering components.

- **Ordering Components:**
  This time is for contacting different companies and placing orders.

- **Building Test Rig:**
  Once all the components have arrived, the creation of the test rig will start.

- **Verification of Test Rig:**
  When the test rig is completed, it will have to be tested and verified to see if it works properly.

- **Written Report:**
  Fragments of the study as it progresses will continuously be added to the final report.

- **Preparing Presentation:**
  This time is for making the presentation of the whole project.

3. Theory

3.1 Wear

Study of the literature revealed that wear, was and still is, not an exact science. Different authors use slightly different types of equations to describe wear and have different ideas on how it acts. Therefore, trying to figure out what type of wear that affects the wheel and track configuration by only going through literature would be a difficult task. Also most studies that are available and similar, covers train wheels and railroads. Not entirely different but it would be inaccurate to assume that the wear is identical. It gives a good platform, but there need to be an examination of the wheel and track to figure out what the differences are.

As for the definition of wear an example can be given that if hydrodynamic lubrication[3] separate two mating surfaces and there is never a direct contact between the two, then the configuration is considered wear free (Dorinson, 1985, pp. 6-7). If a load is high enough to penetrate this layer then wear will exist at the surface. In addition, if no layer is present then subsequently wear will be present.

3.1.1 Wheel and Track Wear

In the wheel and track configuration as it is designed, no hydrodynamic lubrication exists. Therefore, wear is present and a closer look on the different wear types in a rolling configuration was conducted.

Figure 4. Photo of a used carriage wheel to a sliding door.

[3] When a thin film separates two surfaces, this film could even be the atmosphere (Johnson, 1985).

Below is some information on the different wear types that might affect either the wheel or the track. Cavitational wear, impact wear and other kinds of wear that have no or minor effect on the configuration are not covered.

Abrasive Wear:

There are two different types of abrasive wear, two-body and three-body wear. Two-body wear occur when a hard surface cuts away material from a softer surface. Three-body wear appears when free particles are acting between the surfaces of two materials. These particles can either be sliding or rolling over the surfaces. The type that removes most material when occurring is usually the two-body abrasive wear (Stachowiak & Batchelor, 2005, pp. 501-527). Because the three-body wear usually coexists with adhesive wear, it can be around ten times slower than two-body wear.

There is a possibility that abrasive wear can be present in the configuration. However, even if large quantities do exist, they will probably only play a minor role in the wear of the wheel and track. This is because abrasive wear occurs mostly during sliding conditions, and not with rolling motion when the sliding is very low.

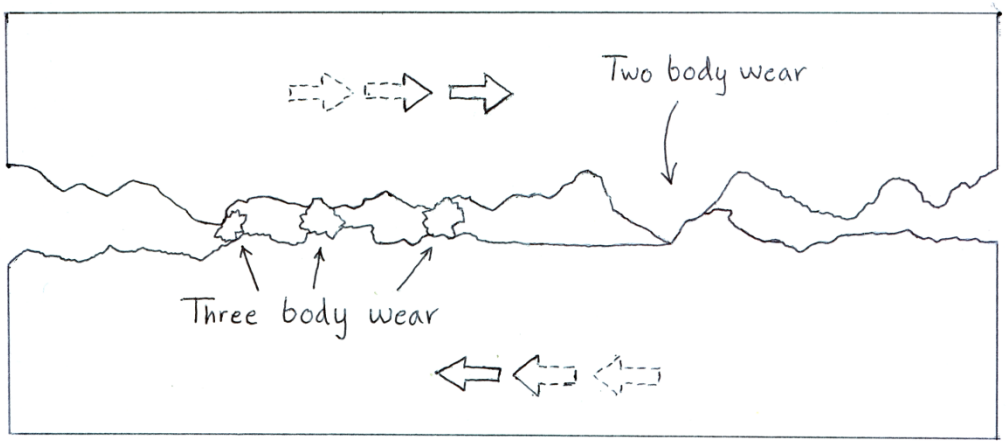

Figure 5. Abrasive Wear

Adhesive Wear:

This wear is present when a high local pressure affects a contact region and the two surfaces are sliding against each other. These high local pressure points exist because the surface is never perfect and contains asperities[4]. The asperities are plastically deformed and later become welded together, tearing off pieces from one surface to the other.

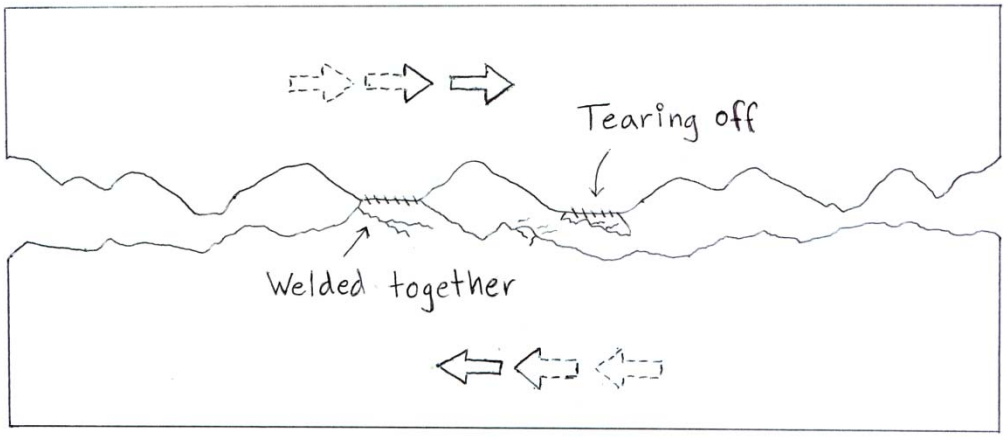

Figure 6. Adhesive Wear

Corrosive Wear:

The best example of this kind of wear is rust, which is a chemical process, created when exposing steel to air creating a thin layer of oxide that forms on the surface. The layer thickness depends of temperatures and material properties. Because the wheel and track never experiences temperatures that are over 200 °C the oxidative layer will be very thin, and makes it easy to break. Wear occur when oxide layers falls off and becomes replaced by new layers of oxide causing material loss. If the object is moving against something, then the sliding speed is also an important factor to determine how effective the wear is.

The oxides created on the surfaces are usually more brittle than the underlying material; therefore, the creation of cracks will become more frequent and spread down to the original material making big pieces of material fall off.

Extensive wear could occur in the wheel and track application if it is not protected enough against the weather or other sorts of corrosives. This could be an important factor requiring consideration.

[4] Small projections from the surface like a point or bump.

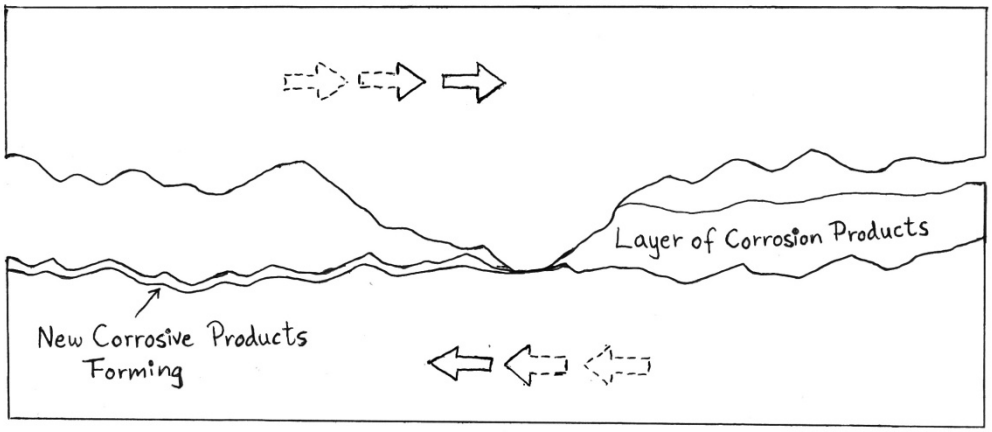

Figure 7. Corrosive Wear

Fatigue Wear:

Fatigue wear is the most dominant wear during rolling (Stachowiak & Batchelor, 2005, pp. 603-614). This kind of wear is present because of the high local contact stresses that create tension in the material. Fatigue wear occurs when a surface experience cyclic deformations or stresses. These cycles create cracks under the surface, which eventually propagates and intersects with the surface. This creates wear particles, which falls off by further cycles and result in a progressive loss of material from the already worn surface.

According to Bayer, the amount of fatigue wear at a surface is proportional to ratio of contact pressure to compressive yield stress. This, theoretical models and empirical observations suggest that amount of fatigue wear is

$$V = KP^n S, \qquad n \geq 1 \tag{1}$$

Where P is compressive load and S is the number of revolution for rolling situations. K and n depends on a range of material and contact parameters, which have to be extracted form laboratory tests (Bayer, 2004, pp. 51-54).

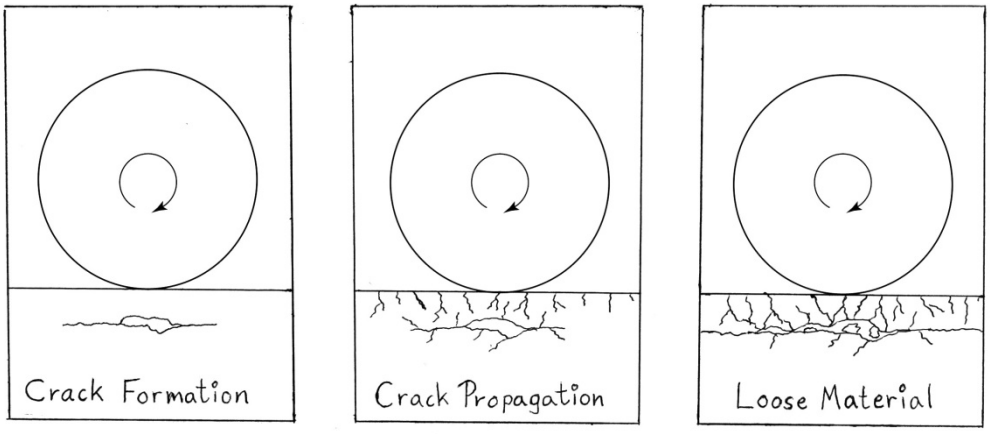

Figure 8. Fatigue Wear

Another empirical relation for fatigue wear called Palmgren's equation where N_1 is the number of revolutions required for a load of P_1 and N_2 the number of revolutions required for a load of P_2. The value of n depends on contact situation where in point contact n is 3 and in line contact n is 10/3 (Bayer, 2004, p. 41) (Seherr-Thoss, Aucktor, & Schmelz, 2006, p. 113).

$$N_1 P_1^n = N_2 P_2^n \tag{2}$$

With the equation, a higher load used for a shorter time can predict how many revolutions a lower load will be able to sustain.

Fretting:

This type of wear occurs when two surfaces in contact during load have a small amplitude oscillatory motion in between them. These small motions and a heavy load creates rubbing on the surface that causes damage. This leaves the possibility that fretting could be forming when the wheel is in contact with the track.

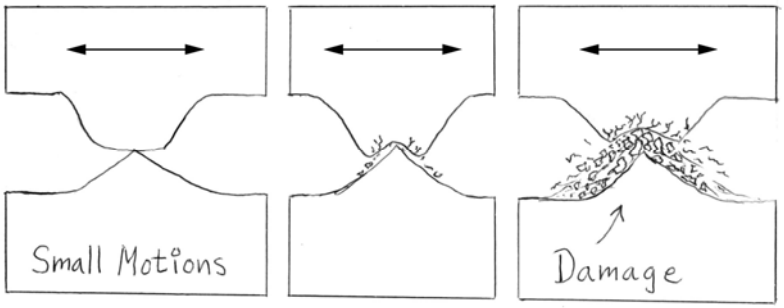

Figure 9. Fretting Wear

3.2 The Hertz Theory

When pressing two solids with perfect spherical or ellipsoidal surfaces against each other without deformation, the contact area would be infinitely small. This in turn would lead to an infinitely large pressure, in view of the fact that the pressure equals force divided by area. To avoid gaining this physical impossibility different types of deformations need special consideration. When the two solids deform they create a larger contact area that spreads out the pressure making it smaller. This type of deformation including how the pressure is changing over the contact surface was what Heinrich Rudolf Hertz described in his work (Jacobson & Vedmar, 2006).

The pressure within an ellipsoidal contact that Hertz developed is as follows:

$$p = p_{max}\sqrt{1 - \left(\frac{x}{a}\right)^2 - \left(\frac{y}{b}\right)^2} \tag{3}$$

Where a and b, see Figure 10, are radii of contact ellipse in the x- and y-direction. The volume of the half ellipsoid represents the compressive force applied to the contact. With this, it is possible to extract the maximum pressure:

$$P = \frac{1}{2}\frac{4}{3}\pi ab p_{max} \implies p_{max} = \frac{3P}{2\pi ab} \tag{4}$$

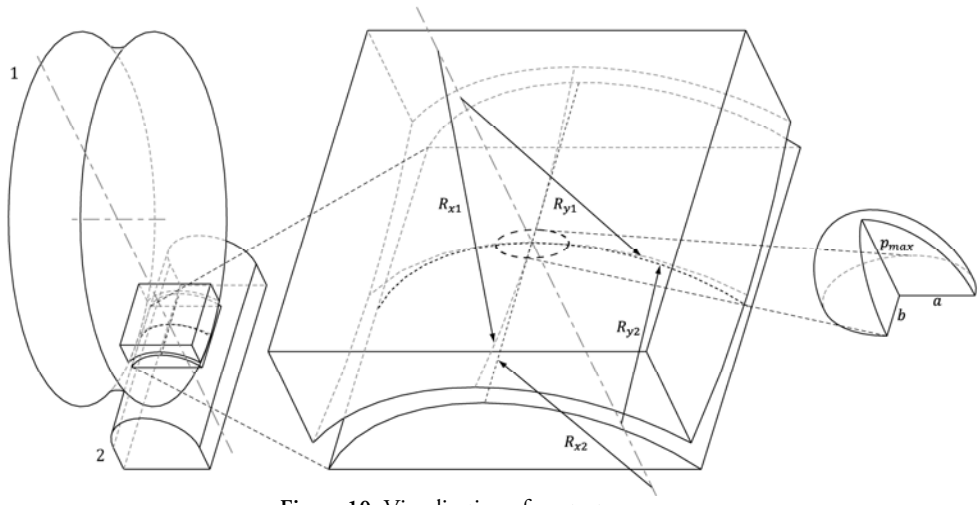

Figure 10. Visualization of contact pressure.

Detailed equations used to calculate contact pressure, deformation, major and minor semi-axes of contact ellipse a and b are available in Appendix A.

3.2.1 Contact Stress

The pressure introduced by the deformation of a point or line contact creates stresses in the material that are three-dimensional. These are often called Hertzian contact stresses since the equation of contact pressure were developed by Hertz (Shigley, Mishke, & Bydynas, 2003).

Stresses introduced repeatedly, e.g. rolling situations, may result in fatigue wear if the stresses are large enough. The most critical type of stress for this to happen is shear stress (Stachowiak & Batchelor, 2005, p. 289), and it is possible to calculate its maximum point using the principal stresses. As long as the value of major- and minor semi-axis *a* and *b* is about the same, i.e. circular contact, the principal stresses is easy to calculate otherwise it is more difficult.

Detail equations on how to calculate the principal stresses and maximum shear stress are available in Appendix A. Figure 11 show stress result of two steel spheres pressed together.

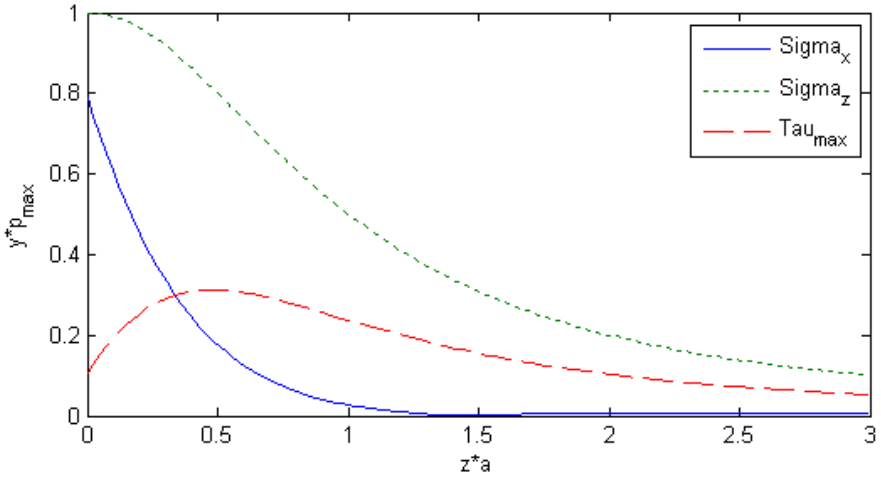

Figure 11. Principal stresses and maximum shear stress.

4. Theoretical Model

4.1 Method

Two steps were used in the creation of the theoretical model, first a verification of the wear and then the creation of a mathematical model. The wear was verified by using a microscopic analysis, which is a good method of deciding the different kinds of wear that might be present. With the mathematical model, there will always be a problem in deciding how deep and detailed it should be. There is no limit to how detailed a model can become, but the more detailed it is the more time it will require to complete and time is always valuable in any project.

For the study two different types of wheels were examined, one with a plastic surface on top of aluminium and the other made of solid steel. In addition, the nylon tracks that are used with the wheels were also studied.

4.1.1 Verification of Wear with Microscopic Analysis

The verification process was made with the aid of microscopes by examining samples of used steel wheels, plastic wheels and nylon tracks. The goal was to find out what types of wear that affects the different parts. The two different wheel configurations used for the study are in Figure 12.

Figure 12. Photos of the two examined wheel types.

The samples were prepared before the microscope could use them. They were disassembled form their attachment system and cut in half by a hacksaw. Consideration was taken to prevent contaminating the samples with metal particles, but the disassembly did not take place in a strict laboratorial environment so some contamination was found on the surface. Due to the shape of the track, it was less affected of contamination when cut into pieces.

Figure 13. Prepared samples.

During the examination of the samples, they were first inspected in their current condition after which they were cleaned in order to see what was below the layer of smudge formed on the surface.

The examination was done with two microscopes, one with a magnification of up to 50x (LECIA DMRME) and one for a more overall view with better lightning (LECIA MZ16).

Figure 14. Microscopes, DMRME to the left and MZ16 to the right.

4.1.2 Creation of Mathematical Model

The mathematical model was created with the knowledge gained from the literature study and the final verification of the microscopic analysis.

The mathematical model was divided into sub-stages that focused on different problems which arose during the study. These were:

- **Input Values:**
  All needed values for the models such as wheel and track dimension, material data and more.

- **Fatigue Wear:**
  From the wear theory, the most dominant wear in rolling situations (Fatigue wear) contained equations to calculate the amount of wear.

- **Optimization of Wheel and Track:**
  Present maximum contact pressure used as an optimizer for better wheel and track combination.

- **Temperature rise in Wheel rolling:**
  When a wheel rolls some sliding will occur at the contact point, this will generate friction heat thus increasing the temperature of the whole wheel.

- **MATLAB**:
  Software used for calculations and visualizations.

Input values

Before any mathematical model could be created some dimensions and data had to be found. Dimensions from the existing wheel and track were obtained from the cooperative company. Material data such as Young's Modulus and Poisson's ratio for the steel wheel were set to standard values. The rest were found at external references.

Table 1. Input values for standard configuration.

	Steel wheel (1)	Nylon track (2)
Rx	22.5 mm	∞
Ry	7.25 mm	6 mm
Young's Modulus (E)	200 GPa	1.59 GPa (*)
Poisson's ratio (ν)	0.29	0.39 (*)

(*) Nylon PA 66 (Callister, 2007)

Fatigue Wear

The theory of Fatigue Wear contained two equations. Equation (1), see page 12, predicts the volume of fatigue wear that would appear from a lifecycle of a sliding door. The amount of test results this equation required made it hard to use. Equation (2), see page 13, on the other hand required minimal amount of data and test results. Because of this, the calculation of wear used only Palmgren's equation.

Palmgren's equation uses number of revolution in its calculation. However, one sliding door cycle consist of a certain amount of revolutions. Therefore, number of cycles was used instead of number of revolutions for the equation. The difference in wheel sliding per revolution with another load was considered negligible.

Optimization of Wheel and Track

The theoretical contact pressure at a certain load, wheel and track combination could be use as a reference pressure for other combinations with the same material but other dimensions of radii and the amount of force.

The allowed combinations of wheel and track radii were based on existing wheel and track radii. These were used as boundary conditions for which the radii could variate within. For example, the largest radius (*Rx1*) was allowed to be between 15 mm and 22.5 mm. To get similar contact situation some limits had to be set in relation to the reference combination.

- Maximum pressure was allowed to differentiate within 5%
- The value of *a* (major semi axis) was allowed to be 5% larger, no lower limit
- Ratio between *Ry1*/*Ry2* was allowed to be 5% larger, no lower limit

In practice lower limit do exist for all the listed limits since the existence of a lower limit for maximum pressure.

The reference combination that was used for the optimization was; a load of 500N (current maximum load), standard steel wheel and nylon track (most common). This produced the needed reference data. The cooperative company uses two set of wheel/track combinations but optimization were only done with the most common use combination, steel wheel and nylon track.

Optimization test were done for each 50 N step i.e. from reference load of 500 N to 150 N. All radii's step length was set to 0.25 mm to minimize the number of combinations and in a way be larger than manufacturing precision.

Temperature rise in Wheel rolling

When wheels roll a small amount of friction occur that increases the temperature in the surface. The maximal increase of temperature can be calculated if the heat flow is constant as (Ertz & Knothe, 2002):

$$\Theta_{\max} = 1.253 \frac{\varepsilon \mu v_s p_{max}}{\beta_w} \sqrt{\frac{a}{v_w}} \qquad (5)$$

Where ε is heat-partitioning factor, μ friction factor, v_s sliding velocity, β_w thermal penetration coefficient and v_w wheel and sliding velocity.

MATLAB

With the use of the MATLAB software, it was possible to create a better view of how the pressure and contact area changes with different types of radii on the wheel and track. The platform has a programming language with an easy interface for inputting different types of calculations. To calculate the various equations it uses a numerical computing process. With an access of a lot of pre-programmed code, this makes calculations and visualizations easier like plotting different graphs. It also contains different special functions ellipke[5], fzero[6] and ezsurf[7]. Those helped in the process of generating the different results.

[5] EllipKE(M), returns the value of the complete elliptic integrals of the first and second kinds, evaluated for each element of M (MATLAB, 2009).
[6] Fzero(fun, x0), tries to find a zero of fun near x0 (MATLAB, 2009)
[7] Ezsurf(fun), Plots a 3-D graph of function fun(x,y) (MATLAB, 2009)

4.2 Results

4.2.1 Microscopic Analysis

What could be seen right away is that a large layer of debris have been formed around the wheel and on the top of the track, which could be the cause that made the sliding door move erratic and create noise. Cleaning both the wheels and tracks revealed no severe wear damage (Vedmar[8]). This brings the conclusion that wear is not an important issue in the lifetime of the sliding doors.

Images of Steel Wheel

Two samples of steel wheels were used, one unused sample to use as reference and one that had been used for 1,365,000 cycles with a weight of 27.5 kg per wheel.

In Figure 15, there is a visible layer of smudge on the surface. The smudge visible on the surface consists of nylon, dust remains or a combination of both (Iyengar[9]).

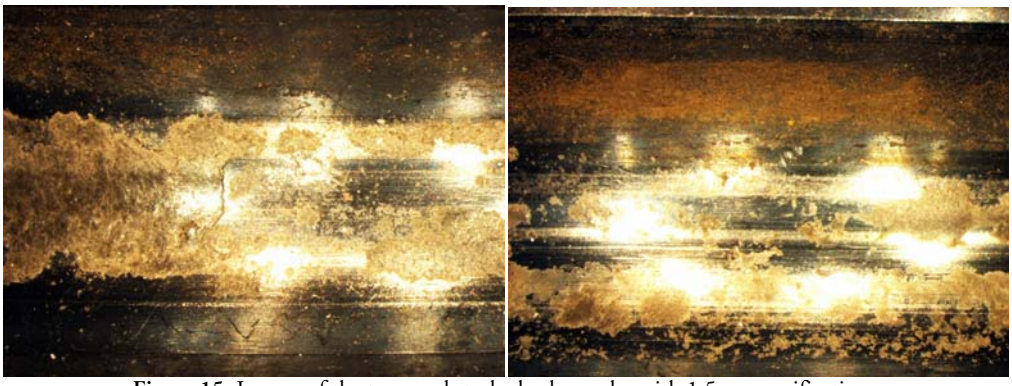

Figure 15. Images of the two used steel wheel samples with 1.5-x magnification.

[8]Lars Vedmar, Assistant Professor, Division of Machine Element, Lund University, personal call June 4, 2009
[9]Srinivasan Iyengar, Associate Professor Division of Materials Engineering, Lund University, personal call August 18, 2009

In Figure 16 is a more zoomed-in image of the wheel. Cleaning the steel wheel prior to the enhanced magnification was necessary to get a better look on how the steel surfaces looked like. On the used samples, it was possible to see a beginning of fatigue wear where the surfaces had become coarser. Overall wear seem to have only a minimal effect on the wheel and should not have affected its properties.

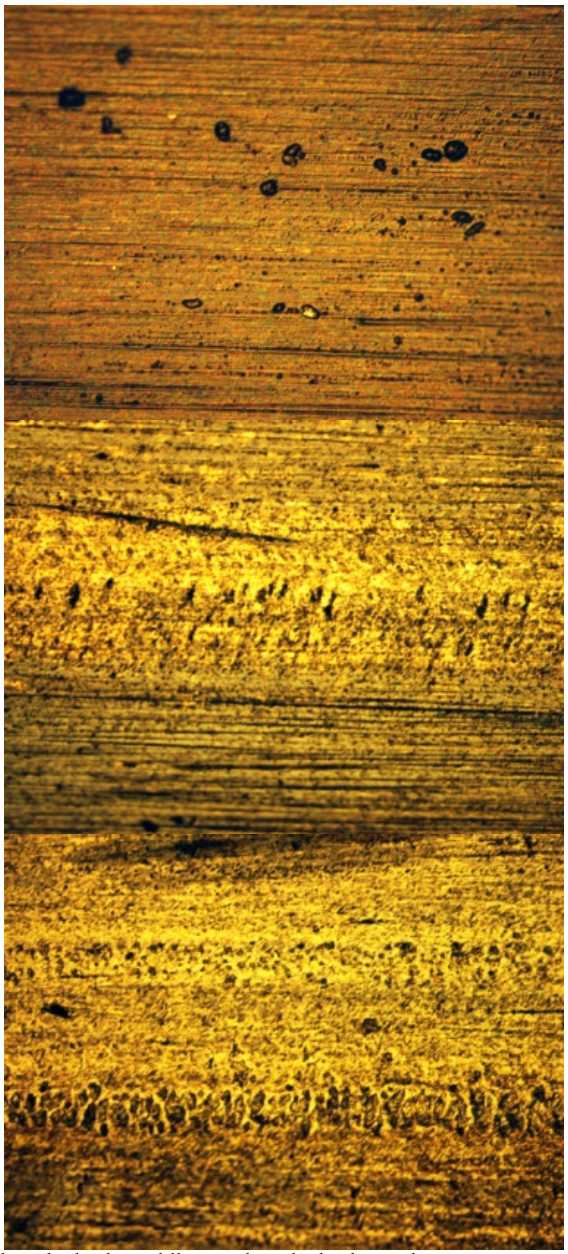

Figure 16. Top: Unused steel wheel. Middle: Used steel wheel sample 1. Bottom: Used steel wheel sample 2. All samples have 10-x magnification.

Images of Plastic Wheel

Two samples of plastic wheels were used, one unused sample to use as reference and one used. It was unknown how many cycles and what weight that had been used on the wheel but enough that some damage was visible for the eyes.

Since the plastic wheels running time is unknown, it is inconclusive to give any statement on how severe the wear is. However, it is possible to see in what direction the wear is taking. In Figure 17, an increase of pitting is visible on the surface and this activity will probably increase over time when the wheels are used.

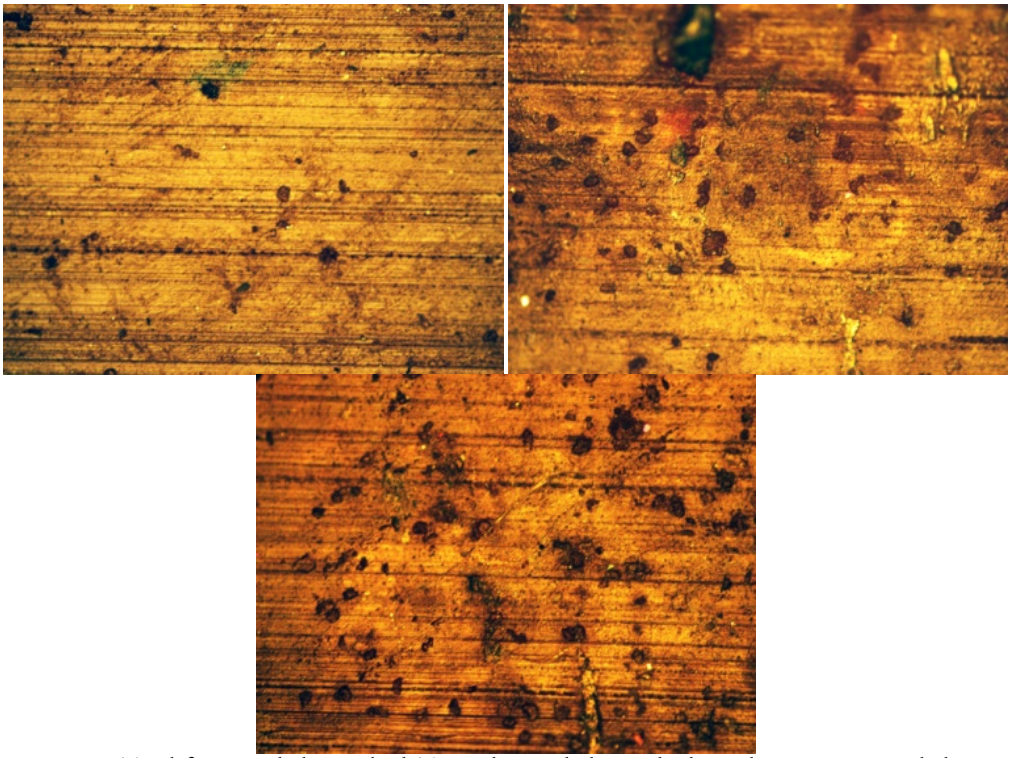

Figure 17. Top-left: Unused plastic wheel. Top-right: Used plastic wheel sample 1. Bottom: Used plastic wheel sample 2. All samples have 10-x magnification.

Images of Nylon Track

Two samples of nylon tracks were used, one unused sample to use as reference and on that had been used for 1,365,000 cycles with a weight of 27.5 kg per four wheels that were pushing down on the track. The nylon track sample are from the same sliding door as the previously studied steel wheel.

Two distinct features are present on the used nylon track, one is smudge probably of the same type as the one on the steel wheel and the other one with a closer look is 45-degree cracks on the surface, both seen in Figure 18. According to Iyengar,[9] the ageing of the nylon and shear stress is the reason for the formation of cracks.

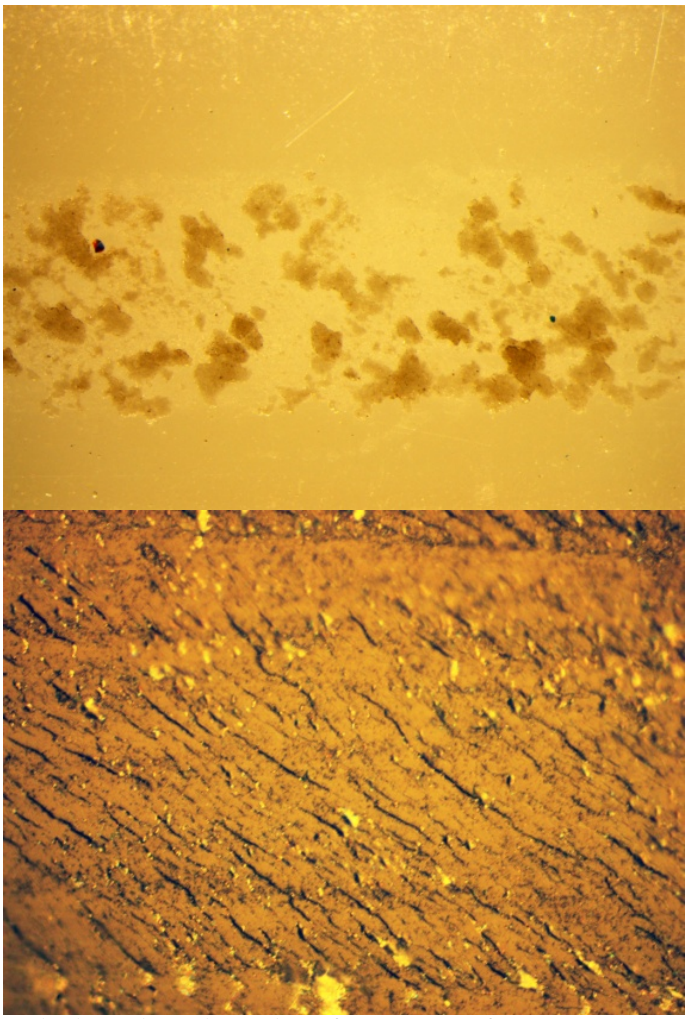

Figure 18. Top: Used nylon with smudge on the surface 1.5-x magnification. Bottom: Used nylon with 45-degree cracks visible on the surface 50-x magnification.

In Figure 19, it is possible to see that there have been big changes on the nylon surface. The straight and clearly visible lines from the unused sample are hardly visible in the one that have been used. In addition, the surface of the used sample has been covered by smudge making the surface more uneven, which could cause noise during usage.

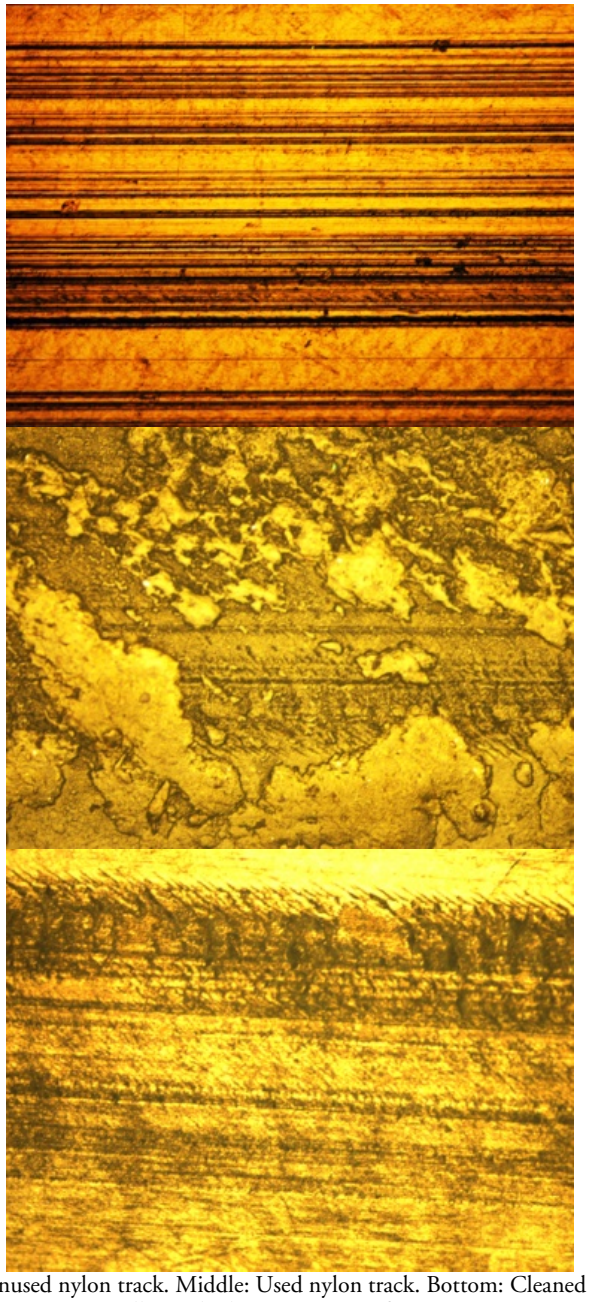

Figure 19. Top: Unused nylon track. Middle: Used nylon track. Bottom: Cleaned used nylon track. All samples have 10-x magnification.

4.2.2 Mathematical Model

Fatigue Wear

The number of wanted cycles of a test was set to differentiate from the reference number to one sixth of the reference. This resulted in rising of the contact force. Figure 20 shows the achieved result, and to cut the number of cycles in half the contact force had to be larger by a factor of 1.26.

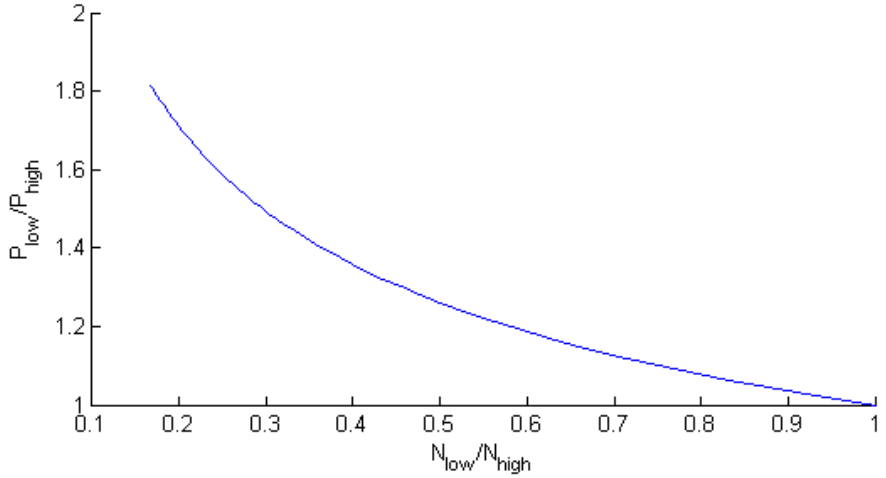

Figure 20. Palmgren's relation.

In addition to higher speed, a test can also be accelerated by applying a greater force. A good combination of both speed and force could cut testing time greatly.

Optimization of Wheel and Track

Before the optimization of radii began the reference configuration needed to be calculated. This were done with the help of MATLAB and the more complex compile equations, called Hertz, found in Appendix A. The result from the calculation are found in Table 2 where δ are the maximum deflection in the contact region.

Table 2. Results for contact of original wheel and track.

	a (mm)	b (mm)	δ (mm)	pmax (MPa)
500 N	2.05	1.54	0.11	75.71

Without changing the wheel and track dimension, it was found that the contact pressure reduces rapidly when the load reduces, which are shown in Figure 21. Different wheel and track combination could then be used for other load cases that are less then 500 N.

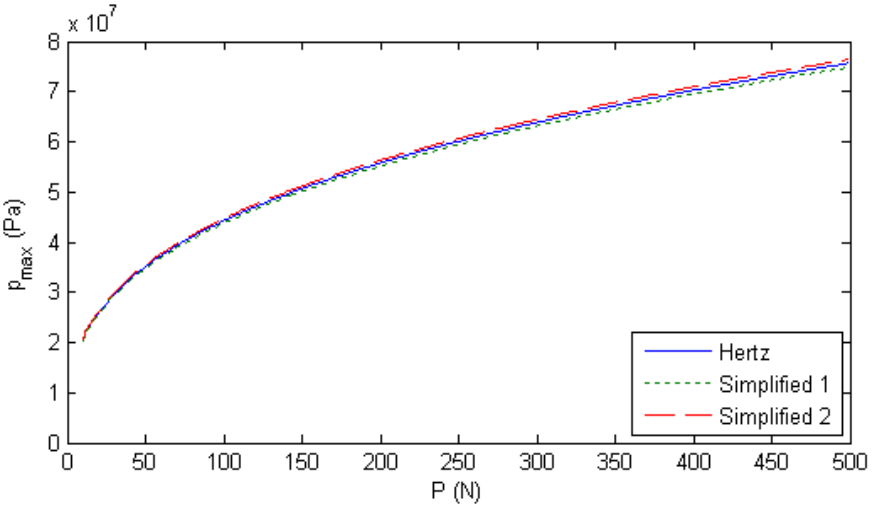

Figure 21. Maximum pressure as function of load (P) for three calculations.

From the calculated maximum pressure of 75.7 MPa (see Table 2), semimajor axis (*a*) of 2.05 mm and the limits allowable maximum and minimum values were set (see Table 3). Since radii of both wheel and track could be changed in between the boundary conditions, one extra limit had to be set. This extra limit served as a radius maximum for the track (*Ry2*) so they never got the same value and became a line contact. Max *Ry2* was set to 0.5 mm lesser than corresponding radius on the wheel (*Ry1*) because of the possibility to calculate and minimize unwanted contact areas. Table 3 shows the final boundary results.

Table 3. Final boundary results.

	Rx1 (mm)	Ry1 (mm)	Ry2 (mm)	pmax (MPa)	a (mm)
min	15	7.25	6	71.9	–
max	22.5	11	10.5	83.3	2.16

With the help of MATLAB, all combination of radii was calculated for each load step. This resulted in 5700 combinations per load. Of these different combinations, some managed to pass through all limits, but in average 150 combinations per load. The load step that had the most combination was 400 N (with 280 combinations) unlike load step 200 N and 150 N where no combination passed. The reason no accepted values were found was that the boundary condition, for the radius *Rx1,* had a lower limit of 15 mm.

Figure 22 and Figure 23 shows the results from the optimization were the chosen combination for each load step was selected with the focus on pressure and ratio limits (see page 20). In Figure 23 the combination have the same ratio and radii (*Ry1,Ry2*) as existing steel/nylon combination. Some of the load steps like 400N show two bars

in Figure 22, this because both passed with very different radii configuration. Detailed data for the charts are found in Appendix C.

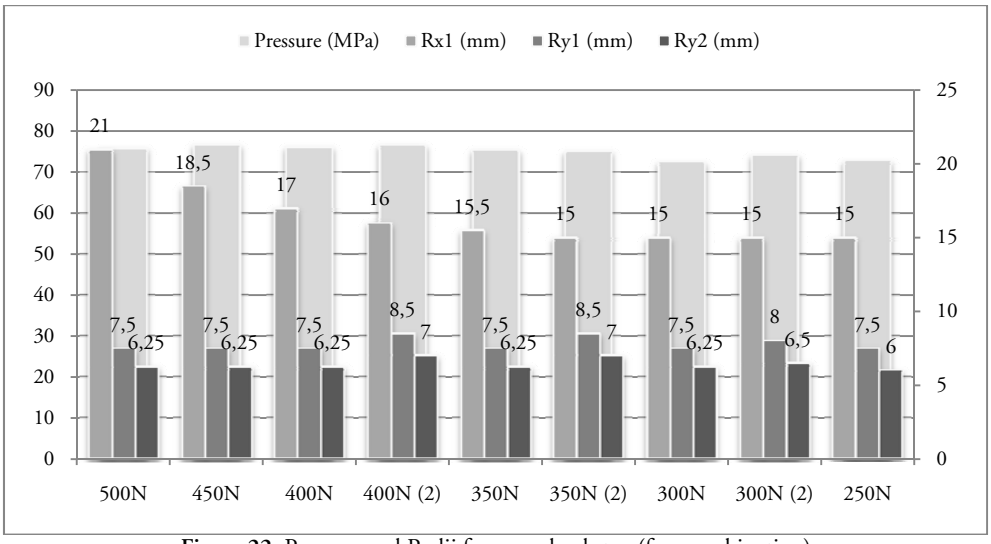

Figure 22. Pressure and Radii for every load step (free combination)
Left gradient – pressure (MPa), Right gradient – radii length (mm).

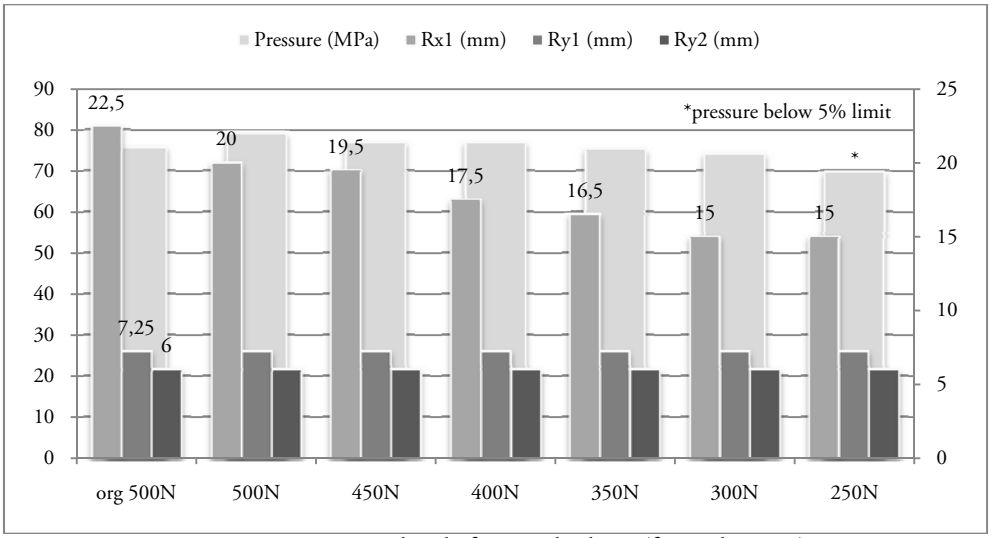

Figure 23. Pressure and Radii for every load step (fix combination)
Left gradient – pressure (MPa), Right gradient – radii length (mm).

Manufacturing accuracy and drawing tolerances reveals that differences in Figure 22 and Figure 23 are slim and only values on the small radii that are similar to original steel/nylon configuration passed. The mainly reason the alternative wheel configuration did not pass was the size of semimajor axis that exceeded the 5 % limit. By changing the radii configuration, the wheel could get up to 55% lesser volume than the original.

Comparison of data for the load 350N showed that the contact area (and maximum pressure) was similar for the free- and fixed-combination (see Figure 24). In the illustration, the surfaces are cut open and the white surface represent the reference contact. More contact illustrations are found in Appendix C.

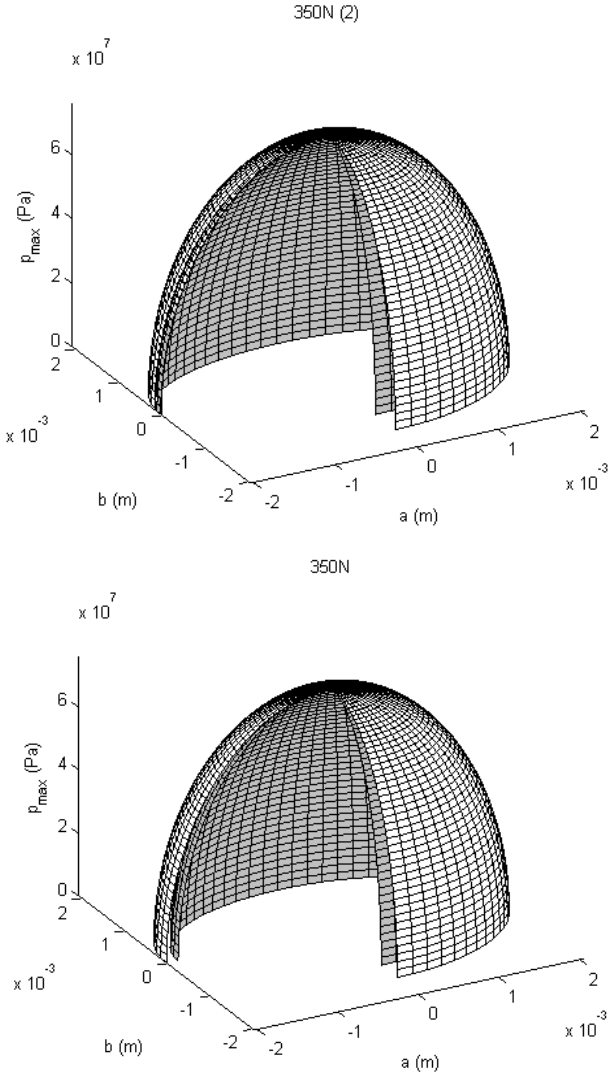

Figure 24. Illustration of pressure by two contact situations
top: free combination, bottom: fix combination.

Temperature rise in Wheel rolling

The Equation (5) to calculate max temperature increase contained many unfamiliar constants that had to be found for the calculation. To see if increase of temperature influences the wheel, non-verified values of all constants and velocities were used. This resulted in a temperature increase of max 2 degrees. Because of this result, no further studies were made with verified values.

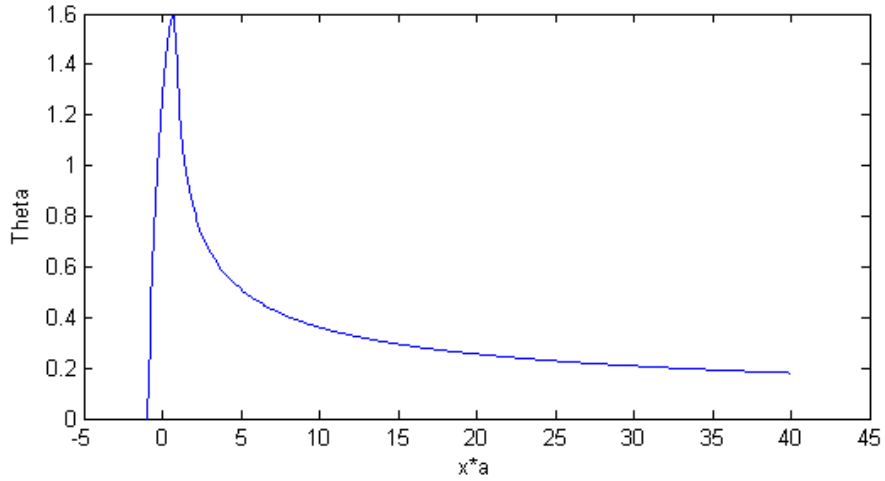

Figure 25. Temperature rise.

4.3 Verification

To verify that the mathematical model produces a reliable result it was decided to use a Finite Element Method analysis.

4.3.1 Finite Element Method Analysis

This analysis was made by using data from given wheel and track properties. The wheel and track was made in SolidWorks[10] and then transferred into the FEM-Analysis program ANSYS.

4.3.2 Geometry

The wheel and track used for the simulation were based on given dimensions of a known configuration used in sliding doors. These dimensions are available in Table 4.

Table 4. Wheel and track dimensions.

	Rx (mm)	Ry (mm)
Track	∞	6
Wheel	22.5	7.25

Optimization of the CAD parts took place to decrease the computing time of the simulation. The optimization was done by removing unnecessary material that has minor impact on the overall results. Based on the calculation the area of contact will be less than 4 mm^2 making it possible to remove more material. The contact area is also symmetrical in the x- and y-direction, therefore a quarter of the material was removed on the basis of symmetry. Changes made to the CAD parts are observable in Figure 26.

[10] Computer-aided design software.

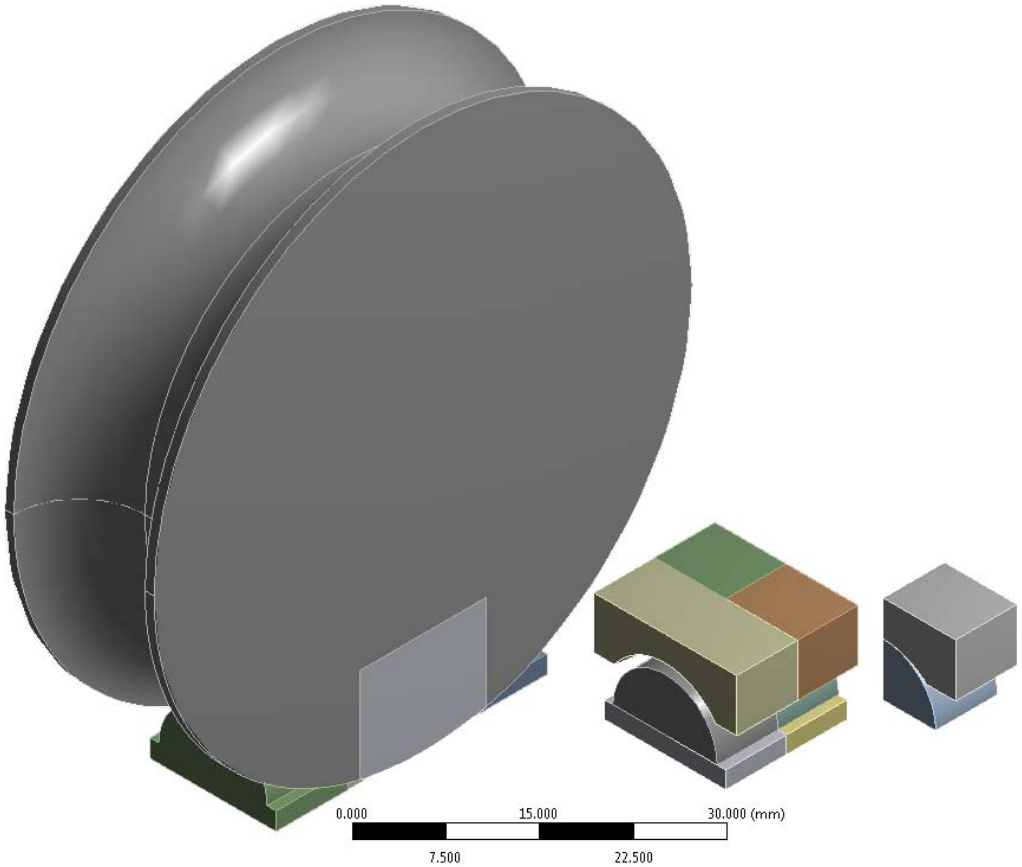

Figure 26. CAD model optimized for FEM analysis.

4.3.3 Material

The wheel is made of a steel material and the track is made of nylon. The material data used for the simulation, presented in Table 5, have values taken from (Callister, 2007).

Table 5. Material data of the wheel and track.

Material	Young's Modulus, E (GPa)	Poisson's ratio, ν	Tensile yield strength (MPa)
Steel	200	0.29	250
Nylon 66	1.59	0.39	90 (70[11])

[11] When wet after storage in a standard 23/50 atmosphere (DIN 50 014) to equilibrium.

4.3.4 Connections

Between the wheel and track, a frictional connection is used. There is always some friction between a wheel and track, which by using the frictional connection presents better results than using a frictionless connection. That is why the frictional connection was chosen even thought the exact amount of friction at the connection point is unknown. The simulation used the maximum friction of a similar nylon.

The formulation in ANSYS was set to Pure Penalty and the interface treatment was Adjust to Touch.

4.3.5 Mesh Structure

The used simulation environment ANSYS Workbench with Academic Teaching Advanced licence has a node limit of 256,000 nodes. In order to create the simulation as accurate as possible the mesh was very detailed in the centre with many node points. By using mesh control of body sizing and then a sphere of influence on the mesh made it more detailed in the centre and less in the outer areas. The final mesh, seen in Figure 27, has the sphere radius set to 2 mm with an element size of 0.05 mm.

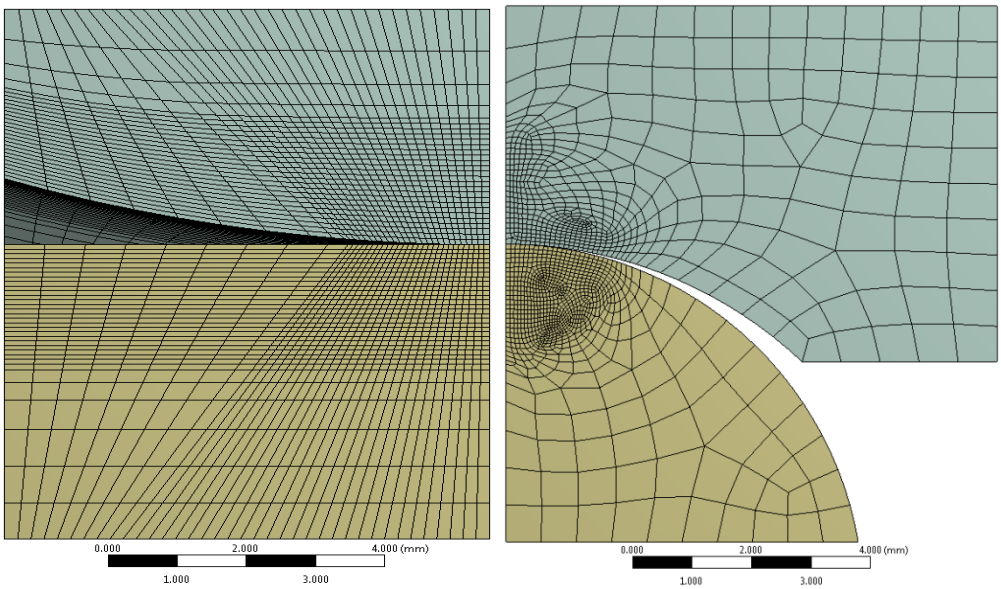

Figure 27. Mesh

4.3.6 Forces and Boundary Conditions

The simulation used the structural analysis option in ANSYS. Fixed support was set on the surface underneath the track. Frictionless support was set on those surfaces facing the side that was cut off because of symmetry, both on the wheel and track. A force of 125 N, one quarter of the original force, was set on the surface on top of the wheel part see Figure 28.

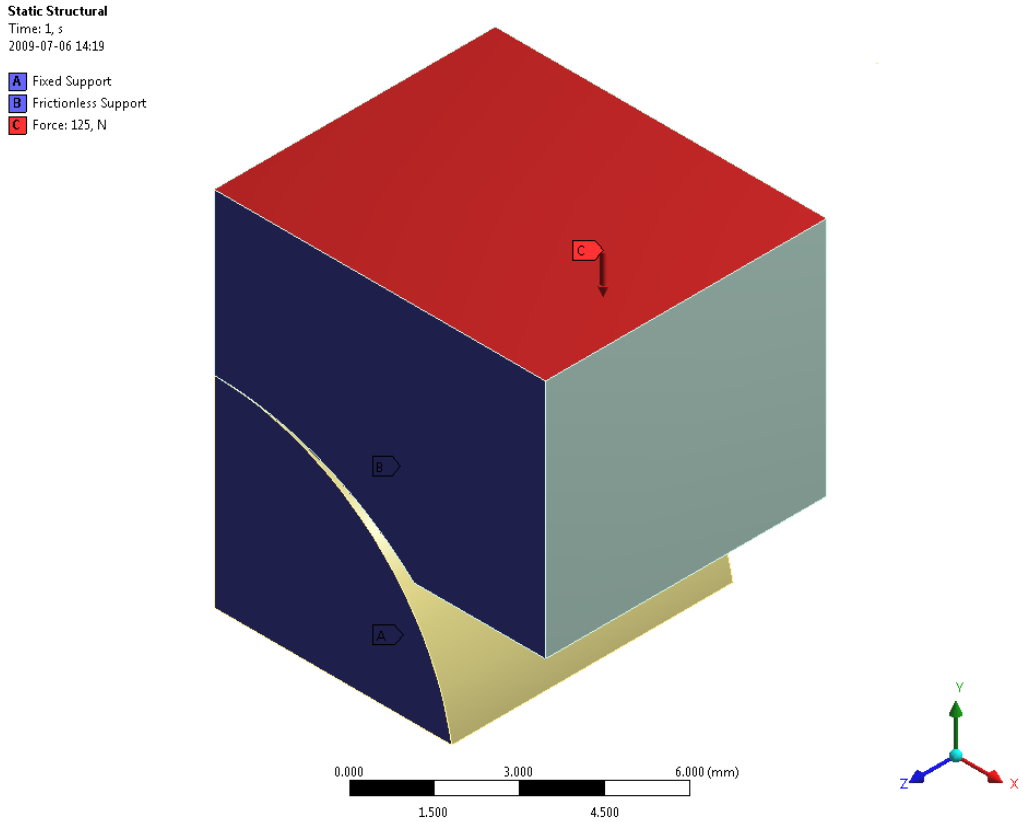

Figure 28. Boundary conditions.

4.3.7 Results

The maximum equivalent stress of 45.7 MPa (shear stress 24.0 MPa) is inside the nylon track and situated about 1 mm below the surface, see Figure 29. In comparison, the theoretical formula gives a maximum equivalent stress of 38.0 MPa (shear stress 21.9 MPa) when converted, with von Mises, from maximum shear stress.

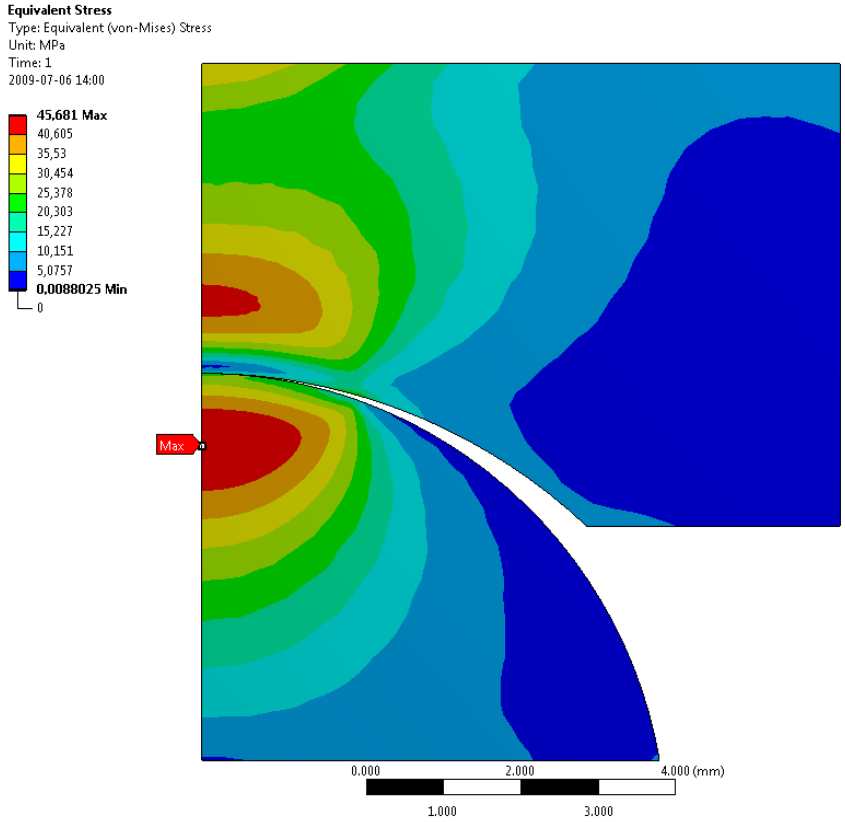

Figure 29. Equivalent stress.

The maximum deformation of the nylon track is 0.09 mm and situated in the centre of the contact point. Calculations from the theoretical model give a maximum deformation of 0.11 mm. Adding deformation in the steel wheel results in slightly increase of total deformation 0.092 mm.

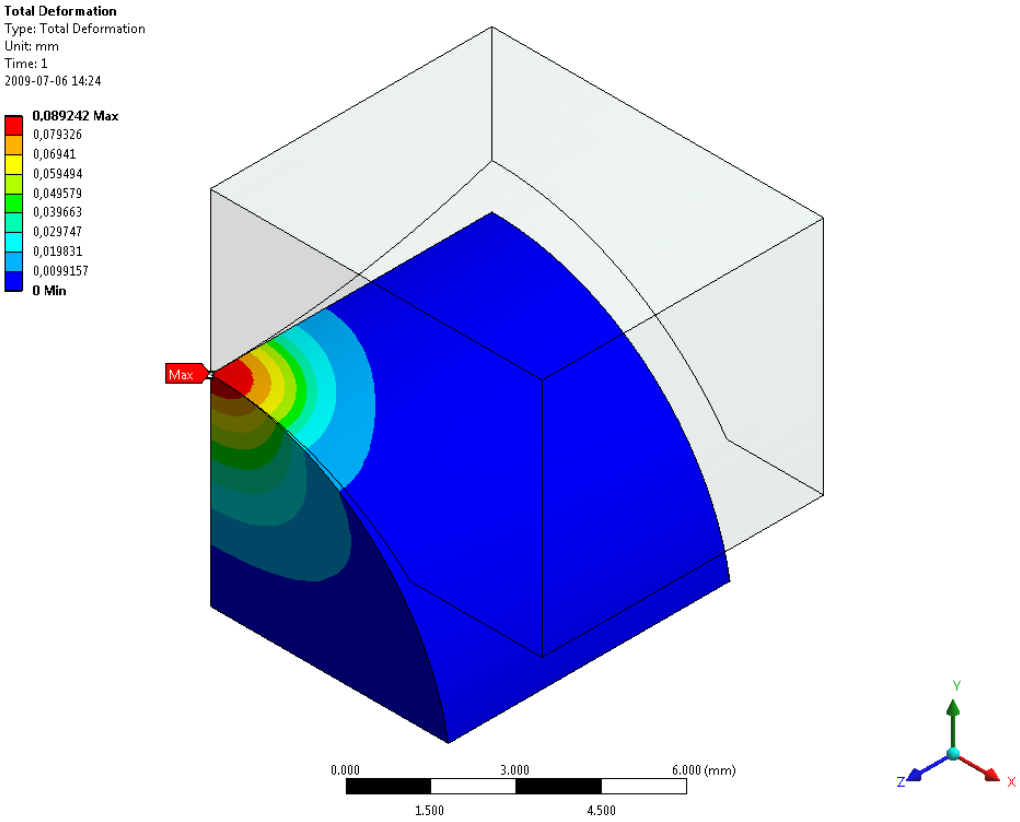

Figure 30. Total deformation.

The maximum pressure experienced on the surface of the nylon track is 78.6 MPa. From Figure 31 the *a* and *b* values measures to 2.0 and 1.6 mm. The theoretical model give a similar result with a maximum pressure of 75.7 MPa and the *a* value as 2.05 mm and *b* as 1.54 mm.

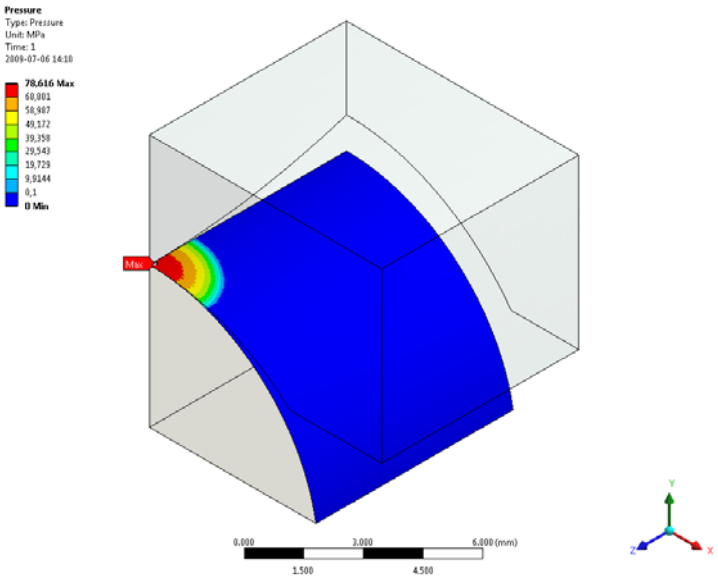

Figure 31. Pressure

The contact status, Figure 32, displays that surfaces that was in contact during the simulation and displayed by the red and orange colour.

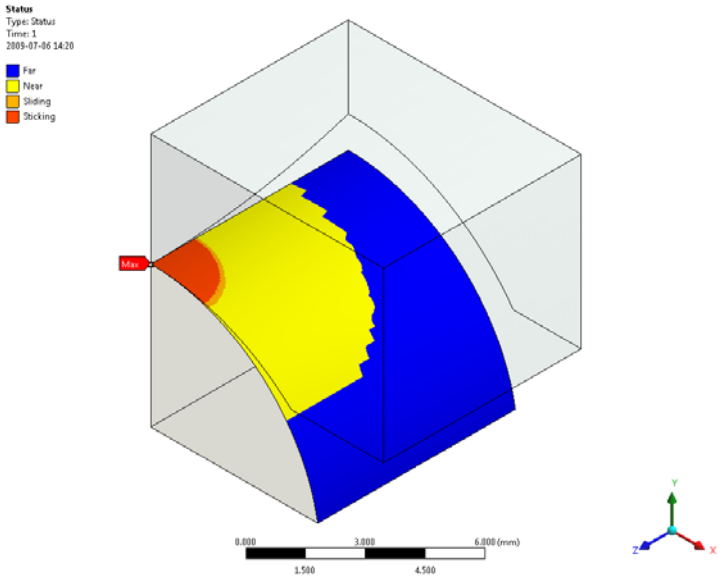

Figure 32. Contact status.

4.4 Discussion

4.4.1 Microscopic analysis

Because the samples displayed no clear visibility of wear, it was concluded that it might not have that big of an effect on the configuration. Nevertheless, it is still hard to leave a final verdict, since not that many samples were tested and those that were only one had a recorded lifetime. ASSA ABLOY Entrance Systems who provided the samples did not have much of a documentary system in place and usually threw away their samples after they have been tested, this also resulted in that the samples available to us was limited.

The wheel and track system that was investigated had not been used at the current maximum load and the wear could be more severe than seen in the samples, but it should still be noticeable what kind of wear that exists and in what level of severity it exists in.

The main problem of long time use seemed to be the gathering of smudge on the wheel and tack, with most covering the wheel. This is the main creator of the noise present when the sliding door gets old after a long usage. When the smudge is removed the noise level returns to normal. Therefore, it should be considered in the design of newer products and a system like an automatic brush that removes it should be put in place.

What actual material the smudge consists of could not go into any detail since the necessary equipment was no available at the time. A more detailed study on this matter should be made and it is highly recommended to do. This will ensure that the problem will be fully understandable and how to avoid it being formed.

4.4.2 Mathematical model

The first preparation and study was based on making a mathematical model that could calculate the volume of mass lost during a specific time due to wear. With the microscopic analysis, it was concluded that wear was not the major issue. The development of the mathematical model took a new direction and it was decided that it should be able to calculate how much load a specifically shaped wheel or track could handle before it risks being overloaded. In addition, by being able to change and optimize the dimensions create a wheel that weight less and require less material thus being cheaper, but still can handle the same amount of load.

The current model could be updated with an equation covering the use of multiple layers of materials (Johnson, 1985), but because of the timeframe, it was never fully implemented and will be left to future studies.

A control of Palmgren's equation should also be made with a real test to see if everything functions as expected. Overall the mathematical model will work as a good base for more advanced versions made in the future, with functions like demonstrating how the nylon becomes weakened with ageing or fatigue that is created during prolonged use that could be added later.

4.4.3 Verification

The theoretical model gives similar values to the finite element method analysis. Even though the analysis never can reflect the reality fully it does give a good approximation that gives validity, and it is sufficient as a verification of the theoretical model. The comparison of the results from the mathematical model and the FEM analysis showed that the mathematical model could be considered valid, since the mathematical equivalent stress only included maximum shear stress and the FEM analysis included all stresses. Although a further test would be good to do to compare how well it is compared to a wheel and track working in a real sliding door. Also in this test, the rise of temperature in the wheel could be made as a verification of the assumption.

5. Practical Device

5.1 Method

The structure used in the development, based on the Ulrich and Eppinger method, had some modification to fit the purpose and time schedule of the project. Overall it followed the standard steps and further information about the method is available in the book "Product Design and Development" (Ulrich & Eppinger, 2008).

The following steps are included in this development process:

1. **Product Specifications:**
   These specifications are important to have in the beginning before the start of any design or engineering. They present what kind of performance that developers are expecting of the new product. It can be hard to set a final specification list in the beginning of a project and changes to it during the development are common, this to make it more realistic to reach the goal. In the start of this study a set of requests were set and translated into specifications. These specifications are of what kind of performance that would be preferred for the new type of test rig. Generally, the aim is to make the new test rig better than the former one, and therefore the old test rig is good to have as a benchmark to bring up its strengths and weaknesses.

2. **Concept Generation:**
   In this part as much ideas as possible are brought up to create a set of different types of concepts. The concept displays a simple view of how a function should to work and presenting them in the form of sketches are usually the best way. Enough time in the concept generation process should be taken that all possibilities are considered, this will reduce the risk of a better design being discovered later in the process.

3. **Concept Selection:**
   The purpose of this step is to evaluate the different concepts by comparing how they might perform depending on different criteria or by simply making a personal choice. There are many different ways on how to choose which concepts to continue working on; for example, by an external decision making the company choose which one it likes the most, or simply by intuition, voting and prototype testing. In this case, the decision was to use decision matrices that give a more objective selection process.

4. **Final Concept:**
   After the winning concepts are selected, it is time to combine them into a final concept. This creates new problems that have to be solved in order to create a functional product. Components that will carry out the functions have to be found and built together.

5. **Concept Testing:**
   When the final concept is created, it has to be tested to find out if it will function in reality before the first prototype is created.

6. **Prototype Finalization:**
   Once the concept testing is completed the final touches on the prototype model is made. This is done by checking that the concept will be able to work together with the outer environment. For example, some things that are not specifically connected to the winning concept but still required to make the whole product work.

7. **Prototype Design:**
   In this phase, the whole design for the prototype should be finished and the only remaining thing should be to order components and build the prototype.

8. **Prototype Testing:**
   Once the prototype is finished, it has to be tested to see if it will be able to function as required.

5.2 Product Specifications

5.2.1 List of Metrics

A list of metrics was created before the benchmarking, this will ensure that it will be easier to study the product needs. Most of the metrics are created for the objectives given at the start of the study, but also from experience that was gained during the development.

Table 6. List of Metrics.

No.	List of Metrics		Product Needs	Imp.
1	Ability to measure	The test rig	provides an easy way of measuring the force.	3
2	Cost of Manufacture	The test rig	is cheap to build.	2
3	Cost of Reuse	The test rig	is cheap to reuse.	4
4	Ease of Configuration	The test rig	uses a simple way of changing the force.	3
5	Ease of Manufacture	The test rig	is simple to build.	1
6	Force Dispersion	The test rig	has a minimal resulting force to the surroundings.	3
7	Realistic Behaviour	The test rig	behaves similar to a sliding door.	5
8	Simplicity	The test rig	is built using simple components.	3
9	Use of Space	The test rig	is compact and does not take much space.	3
10	Wear Acceleration	The test rig	can cut testing time by accelerating the wear.	5
11	Wear Similarity	The test rig	makes the same type of wear present on sliding doors	3
12	Weight	The test rig	has a light moving mass.	4

5.2.2 Benchmarking

The current wear testing rig used by ASSA ABLOY Entrance Systems was set to be the benchmarking product. Its main functions were examined and inspired ideas during the concept generation. It was used as the reference during the concept phase to help get a better evaluation of the different concepts.

5.3 Concept Generation

The problem is decomposed into simpler sub-problems to make it solvable in a more focused way. The approach used to divide the problem was by sequence of important functions, and this option is selected to get a broader view of the simple problems that the device consists of. Figure 33 illustrates the different sub-problems selected.

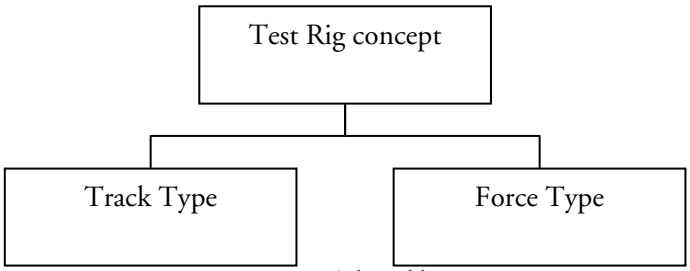

Figure 33. Sub-problems

- **Track Type:**
  Concepts of different shapes of the track and how the wheels are placed.
- **Force Type:**
  Concepts how to achieve contact force.

To find solutions to the sub-problems identified, a research of external resources as well as internal (brainstorming) was conducted. External resources refer to detailed evaluation of similar functions and technologies used in products with related sub-functions. Patents and the original wear-testing rig were the two main external sources that were relied upon to reveal existing concepts and to get additional information on the certain strengths and weaknesses of such concepts.

5.3.1 Track Type

0. **Original track:**
   Present state of the track sub-problem lets the wheel travel back and forth on the same track. At the tracks end it has a short pause before it returns to its origin. This cycle continue over time.

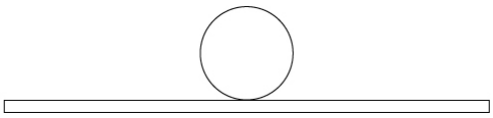

Figure 34. Original track.

1. **Wheel on large hollow circular track:**
   The track curves as a large circular track there the track is the moving part. The inner part of the circular track is hollow or optimized for minimum mass. The wheel presses to the outer surface towards the rotational centre of the track to achieve contact force. The circular shape of the track minimizes the pause and acceleration time since it never has to stop. To simulate back and forth the circular track can change its rotation direction.

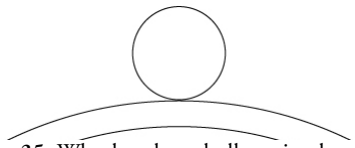

Figure 35. Wheel on large hollow circular track.

2. **Wheel on small circular track:**
   The wheel presses at a track form as a circular track there the track is small but large enough to accommodate several wheels. The small track makes it easy to achieve higher speed. Like in track type 1, the rotation direction changes to simulate back and forth.

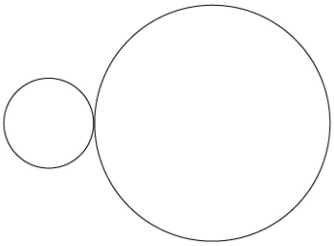

Figure 36. Wheel on small circular track.

3. **Dual wheels on circular track:**
   Two wheels, that are linked together, presses towards each other. A circular track, placed between the wheels, rotates to simulate the motion. As in track type 2, the track is small to get higher speed, but the linking of the wheels ensures low force dispersion to the track's rotational bearing.

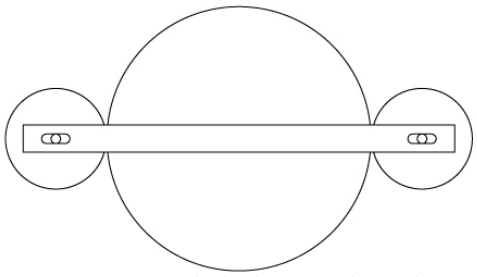

Figure 37. Dual wheels on circular track.

4. **Dual wheels on large hollow track:**
   Two wheels presses together. In between them, a large circular track rotates around its own rotation centre. This linking of wheels minimizes the force dispersion to the tracks rotational bearing. In difference to track type 1, the linking prevents bending of the track, which allows the track to be thinner and lighter. The rotation of the track can be changed to simulate the back and forth motion.

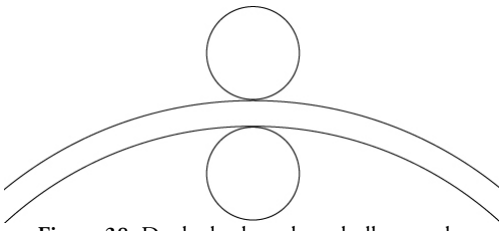

Figure 38. Dual wheels on large hollow track.

5. **Dual original track:**
   Two original tracks placed as if they were mirror in the horizontal plane remove the need of a heavy door. This because then two wheels can be pressed towards each other with the tracks between them. The inertial of the motion reduces since the heavy door no longer exists in the testing. This minimizes the acceleration and deceleration, which fasten testing time.

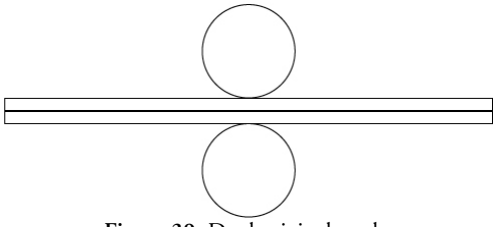

Figure 39. Dual original track.

5.3.2 Force Type

0. **Original force:**
   The original solution of applying contact force uses the same weight as a real door. Alternative force achieves by more or less weight. The inertial motion is high for all doors.

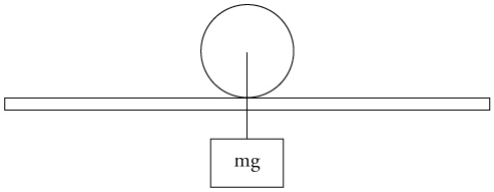

Figure 40. Original force.

1. **Spring:**
   A spring applies the contact force to simulate the original contact situation. Different contact force achieves by changing preload to the spring. This requires a carefully calculated spring constant to get a valid contact force.

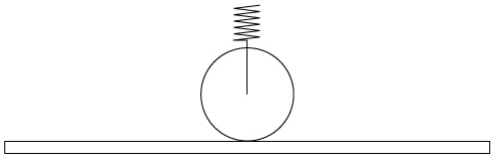

Figure 41. Spring

2. **Pneumatic/hydraulic cylinder:**
   A cylinder, pneumatic or hydraulic, with controlled pressure applies the required contact force. Changing the pressure ensures that different load cases can be made. The cylinder depends on an external compressor with hoses or tubes between them that limiting the motion options.

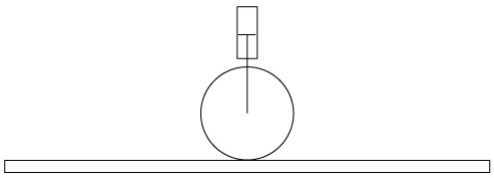

Figure 42. Pneumatic or hydraulic cylinder.

3. **Bolt:**
   A bolt, or nut, forces the wheel against the track by screwing it with a specific amount of torque to the bolt. Different torque results in another contact force. The reliability that correct contact force achieves from the torque, depend on friction in the bolts contact surfaces, subsidence in surfaces and more. This limiting the accuracy of contact force.

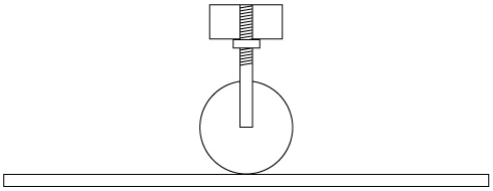

Figure 43. Bolt

4. **Gear:**
   A gear, with a motor attached to it, forces the wheel against the track. The amount of contact force achieves by measure the power to the motor. When the power is right, the motor stops and the contact force remain. Wiring of cables and placing of the motor hardens the potential motion options.

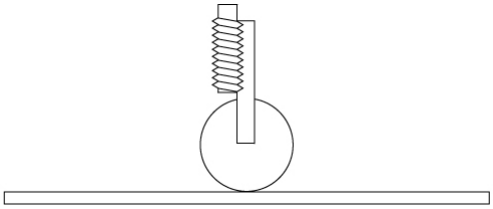

Figure 44. Gear

5. **Electric coil:**
   An electric coil creates a linear motion that forces the wheel and track together. The magnetic flow, and thereby contact force, changes when the current in the coil changes. Since electrical coils needs electrical power wiring and the coil itself limiting the possible motion options.

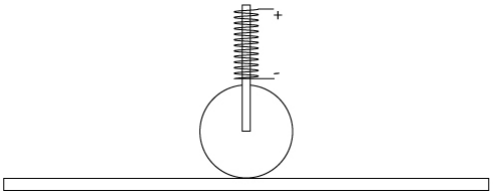

Figure 45. Electric coil.

5.4 Concept Selection

With the generated concepts, the next step was to evaluate them such that a comparison could be made to determine their relative strengths and weaknesses. Ultimately, the goal was to choose the best concept for further development.

Instead of evaluating combinations of concepts, the concepts were evaluated individually within their sub-problem group. The reason for this was that since the solutions from each sub-problem are compatible with solutions from another, an enormous amount of feasible possibilities would appear. To narrow down the options, the best concepts from each sub-problem were chosen by a selection process, and the combination of these top concepts would become the final testing rig.

As a method for choosing a concept, decision matrices were used to evaluate the concepts to a set of selection criteria. In this process, there were two stages: concept screening and concept scoring (Ulrich & Eppinger, 2008), which are supported by these matrices.

To better differentiate between the competing concepts, the concept scoring matrix was used. The criteria for evaluation were chosen as the product needs identified in Table 6 (p. 43), where the secondary needs contained under those primary needs were considered during the ranking. The ranking scale ranges from a value of 1 to 5, where one is the least and five is the most desirable. The relative importance of the selection criteria was weighed, and the concept scores were determined by the weighted sums of the ratings. The weights were decided by the importance of the different objectives for the test rig.

5.4.1 Definition of Selection Criteria

Below is a general description of each selection criteria, both for the track type and for the force type. The weighting decided on each of the selection criteria was based on both what the company thought was important for a test rig and of the study made examining the current test rig.

Track Type

- **Cost of Manufacture:** The cost to manufacture the concept is low.
- **Cost of Reuse:** Cost to make a new test or repair the concept is low.
- **Ease of Manufacture:** To build the concept few new parts have to be manufacture.
- **Force Dispersion:** The resultant force from the concept to its surrounding is small.
- **Realistic Behaviour:** The concept test environment is similar to reality.
- **Use of Space:** The amount of space the concept requires is low.
- **Wear Acceleration:** Wear appears faster than in reality.
- **Wear Similarity:** Wear that appear from the concept is similar to reality.

To make the evaluation more accurate a list of importance for the weighting method for the different selection criteria came into place. These will be shown in the order of importance: Realistic Behaviour (5), Wear Acceleration (5), Cost of Reuse (4), Force Dispersion (3), Use of Space (3), Wear Similarity (3), Cost of Manufacture (2) and Ease of Manufacture (1).

Force Type

- **Ability to Measure:** Measurement of the contact force is easy.
- **Cost of Manufacture:** The cost to manufacture the concept is low.
- **Ease of Configuration:** Setup of the concept is fast and easy.
- **Realistic Behaviour:** The concept force behaviour is similar to reality and small variations have a minimal effect to the concept.
- **Simplicity:** The concept consists of few parts.
- **Weight:** The concept weight is low.

In the same way as the evaluation of the first sub-problem, the order of importance of the selection criteria was created for sub-problem two: Realistic Behaviour (5), Weight (4), Ability to Measure (3), Ease of Configuration (3), Simplicity (3) and Cost of Manufacture (2).

5.4.2 Concept Evaluation

Once all the criteria have been set the evaluation starts. The different types of concepts were drawn up on a white board and discussions were made on which types were good in which areas. As a reference, the original ASSA test rig was used and the scored were set according to our understanding of how it worked.

Table 7. Evaluation of Track Type.

		Concepts of Track Type											
		0		1		2		3		4		5	
Selection Criteria	Weight	Rating	Weighted Score	Rating	Weighted Score	Rating	Weighted Score	Rating	Weighted Score	Rating	Weighted Score	Rating	Weighted Score
Cost of manufacture	2	3	6	1	2	2	4	2	4	1	2	3	6
Cost of reuse	4	3	12	1	4	2	8	2	8	1	4	3	12
Ease of manufacture	1	3	3	1	1	2	2	2	2	1	1	3	3
Force dispersion	3	3	9	3	9	3	9	4	12	5	15	5	15
Realistic behaviour	5	3	15	2	10	1	5	1	5	2	10	3	15
Use of space	3	3	9	4	12	5	15	5	15	4	12	4	12
Wear acceleration	5	3	15	5	25	5	25	5	25	5	25	4	20
Wear similarity	3	3	9	2	6	2	6	2	6	2	6	3	9
	Score	78		69		74		77		75		92	
	Rank	2		6		5		3		4		1	

As can be seen in Table 7 the concept number 5 won, a more detailed description of why will follow:

- **Cost of Manufacture:**
  The Cost of Manufacturing gave it a score of three since it is close to the same basic cost as the reference by using a straight track, creating a circular one will be much more expensive.

- **Cost of Reuse:**
  The Cost of Reuse is similar to the reference since the same type of track configuration will be used and if a new one is needed it can be taken from already existing tracks or produced in the same machine. For the others, if the track have to be changed a completely new one will have to be produced which will result in rising costs.

- **Ease of Manufacture:**
  The Ease of Manufacture have a very low weighting since the amount of tests rigs created will be limited and only for personal use. Since the winning concept will be designed in a similar way to the reference, it was given the same score. The circular track will have a problem of getting a smooth joint transition or if the circular track is made solid it will have to be created by milling, a time consuming task that might require a large machine.

- **Force Dispersion:**
  The less affect the force applied on the wheel to the track will have to its surroundings the better, that is were Force Dispersion comes in. The winning concept gained the maximum score because of the positing of the tracks, which are opposite to each other; this will prevent any bending force on the track.

- **Realistic behaviour:**
  The Realistic selection criteria is how much the track mimics the track of a real sliding door, since both the reference and the winning concept are straight this gives a closer result to reality then the circular ones.

- **Use of Space:**
  The concept with the highest score for Use of Space was the concept 2 and 3; they are the smallest of the concepts and require the least space. The winning concept got a slightly higher score than the reference since it can have twice as much wheel in the same area as the reference.

- **Wear Acceleration:**
  For the potential of wear acceleration, all the circular tracks gained a high score, since it will be easier to create a fast circular motion then a linear one.

- **Wear Similarity:**
  The winning concept got the same score as the reference, since they consist or similar wear surfaces. Rest of the concept got lower score because of the bended contact surface.

Table 8. Evaluation of Force Type.

		Concepts of Force Type											
		0		1		2		3		4		5	
Selection Criteria	Weight	Rating	Weighted Score	Rating	Weighted Score	Rating	Weighted Score	Rating	Weighted Score	Rating	Weighted Score	Rating	Weighted Score
Ability to measure	3	3	9	3	9	5	15	2	6	4	12	5	15
Cost of manufacture	2	3	6	4	8	2	4	5	10	2	4	2	4
Ease of configuration	3	3	9	3	9	4	12	3	9	4	12	4	12
Realistic behaviour	5	3	15	3	15	3	15	1	5	1	5	3	15
Simplicity	3	3	9	4	12	2	6	4	12	2	6	2	6
Weight	4	3	12	5	20	4	16	5	20	4	16	4	16
	Score	60		73		68		62		55		68	
	Rank	5		1		2		4		6		2	

As can be seen in Table 8 the concept number 1 won, a more detailed description of why will follow:

- **Ability to Measure:**
  Both the pneumatic and electric coil concepts have a good potential in providing accurate measures through their system and thus gained the best rating in Ability to Measure. The winning concept, the spring, gained same rating as the reference due to similar measuring method.

- **Cost of Manufacture:**
  With the Cost of Manufacture, the screw concept gained the highest score and the spring came on second place. Both are much cheaper to produce then the reference since they do not require the same amount of material and uses standard components.

- **Ease of Configuration:**
  With Ease of Configuration, the concept should present a simple way of configuring the different forces. The winning concept (spring) and bolt concept got the same score as the reference because they all need a manual adjustment of contact force. The other three contact forces got better score due to the external alteration of force.

- **Realistic Behaviour:**
  The concept should be dynamic and present a force similar to gravity as the real sliding door. The reference is in the same way as the real sliding door, the spring have similar properties and the electric coil thus giving them the highest score. Gear and Bolt concept got low score because of the ability to handle track variations.

- **Simplicity:**
  The spring and bolt gained the highest score because they use simple and standardized components.

- **Weight:**
  To gain a better use of the motor and making the test rig go faster it is better to have the test rig become as light as possible. The spring and bolt gained the highest score since their components will weight the least.

5.5 Final Concept

From concept scoring an identification of the best concepts were made of those that achieved the greatest score for each sub-problem, and the final wear test rig was derived as a combination of those concepts. For the sub-problem "Track Type", the score between concepts one and three are very close, but a decision was made to only choose the top scoring solution because time limits the study to only one prototype. The configuration of the final wear testing rig is as follows:

- **Track Type:** (5) Dual Original Track
- **Force Type:** (1) Spring

5.5.1 Combining the two sub-problems

Once the two different sub-problems are chosen, the next step will be to figure out a way to combine them. The property of the spring gives two possibilities for it to function, either as a expanding or as a contracting spring. The two different types have both pros and cons, in the beginning the expanding spring was used since this gave the simplest and lightest design. After a detailed concept was made a downside was thought about that was of importance namely stability. Since stability is more preferred than the other pros of the expanding spring, a new concept based on the same expanding spring but as a contracting type was made. The contracting type makes the tracks come closer to each other and gives a more similar contact point to the wheels as they work in their usual environment. For better understanding of the two different concepts, see Figure 46.

Figure 46. Two different feather configurations, the one on the left creates a pushing motion and the one on the right contracts.

5.5.2 Creation of the final concept

Once everything was set on how the different sub-problems should work with each other, the next task was to design the model using a CAD environment. For the creation purpose, SolidWorks 2009 was used since the cooperating company is using similar software, having different kind of CAD environments have a big potential to lead to problems in all kinds of development processes.

To make everything work as intended two main mechanisms are put in place, the spring and the sliding that should be fixed to one direction. The dimensions of the springs was decided upon by the specifications given, it have to be able to produce a force of 2000 N. A spring that fit into the given properties was found at Lesjöfors, with a feather constant of 140 N/mm and a feathering deep of 15 mm giving a maximum force of 2314 N. For the linear movement a combination of four LVCR 12-2LS and two LJM12 from SKF was used to stabilize the carriage wheel.

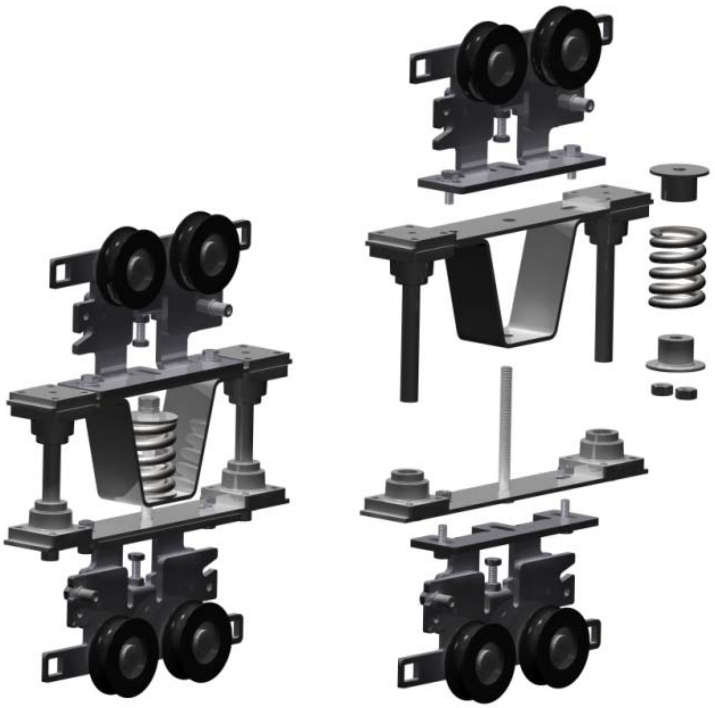

Figure 47. Full assembly of the final concept.

To build everything together as much as possible of original parts from ASSA was used, such as screw dimensions and plate thickness. Drawings and pictures was created of the finalization of the prototype so that the different parts could be designed.

5.6 Concept Testing

It is always important to test if an idea has the potential of working or not before creating the first prototype. One way of doing this is by the use of computer simulations, since a full scale CAD model of the test rig have been created a simulation was made.

When the main function of the rig seemed to work further testing was made with ANSYS, the simulations tested if the smaller components of the rig had the potential of working in a proper state.

5.6.1 Finite Element Method Analysis

This analysis was made by using the CAD models of the winning concept. The models was made in SolidWorks and transferred to ANSYS Workbench for analysis.

5.6.2 Geometry

The original CAD model was broken down and unnecessary components was taken away to make the simulation more efficient and faster. To get a better understanding of how the model looked before and after the optimization see Figure 48.

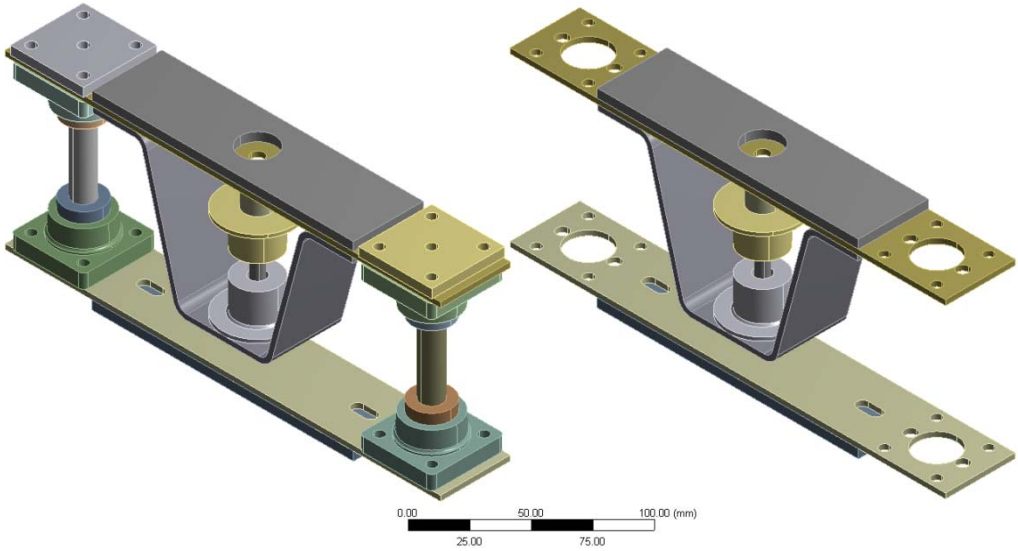

Figure 48. Before and after optimization.

5.6.3 Material

The two plates on top and bottom are made of steel and so are the screw and bolts, the rest of the components are made of aluminium. The material data used for the simulation is presented in Table 9 and the values were taken from the ANSYS standard materials.

Table 9. Material data of the contractor.

Material	Young's Modulus, E (GPa)	Poisson's ratio, ν	Tensile yield strength (MPa)
Steel	200	0.3	250
Aluminium	71	0.33	280

5.6.4 Connections

For this simulation bonded connections was used on the different parts that are connected to each other, those that are not have frictionless connection.

5.6.5 Mesh Structure

To make the simulation as accurate as possible a very high detailed mesh was used. Using mesh control of part relevance on the mesh made it more detailed on the parts with most interest and less in others. The final mesh can be seen in Figure 49, the main holder and the lower feather holder had most part relevance.

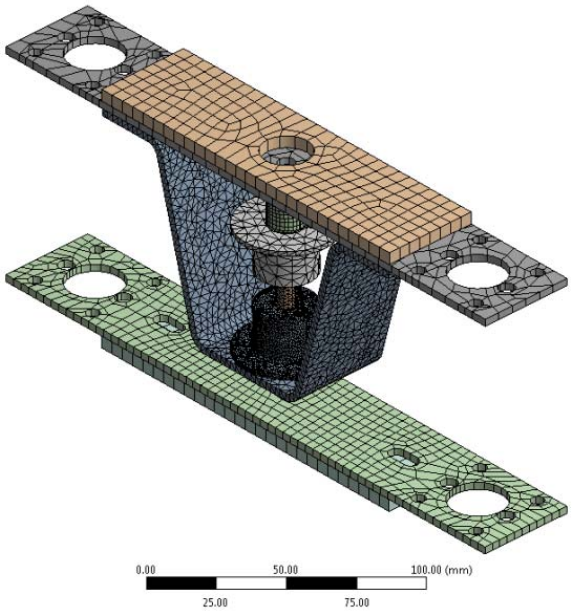

Figure 49. Mesh structure.

5.6.6 Forces and Boundary Conditions

A static structural analysis was used. Fixed support was set on the surfaces on top and on the bottom of the contractor; this is where the wheel is mounted. Frictionless support was set on the surfaces of the big holes in the edges; this is where the linear track is. A force of 2000 N was set on the surface of both the feather holders to give the force of the feather, see Figure 50.

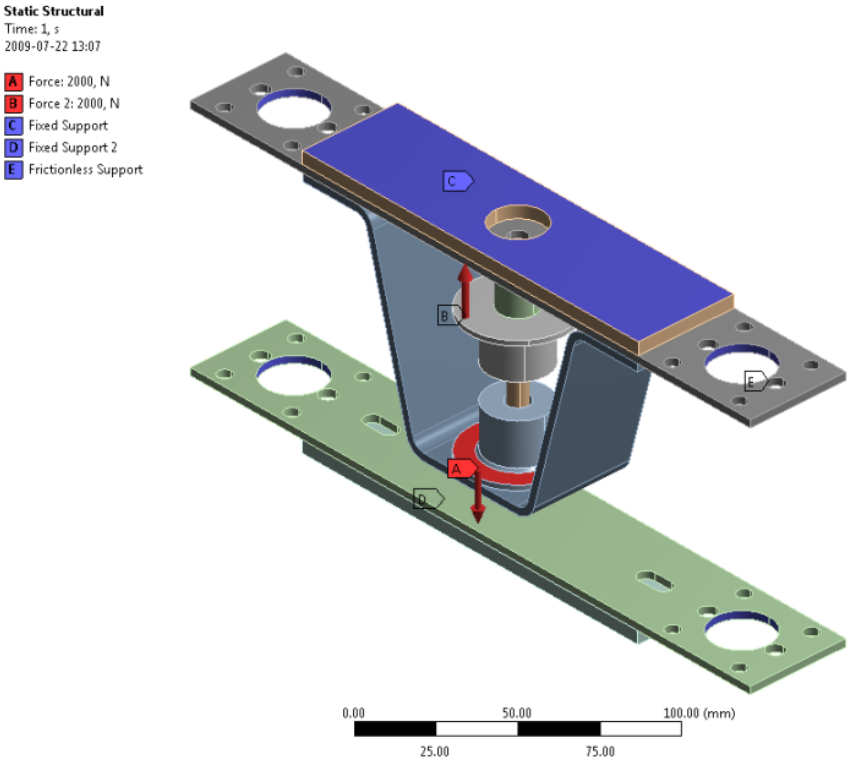

Figure 50. Static structural.

5.6.7 Results

The maximum deformation of the contractor is 0.23 mm and situated close to the contact point of the main holder and the lower feather holder, see Figure 51.

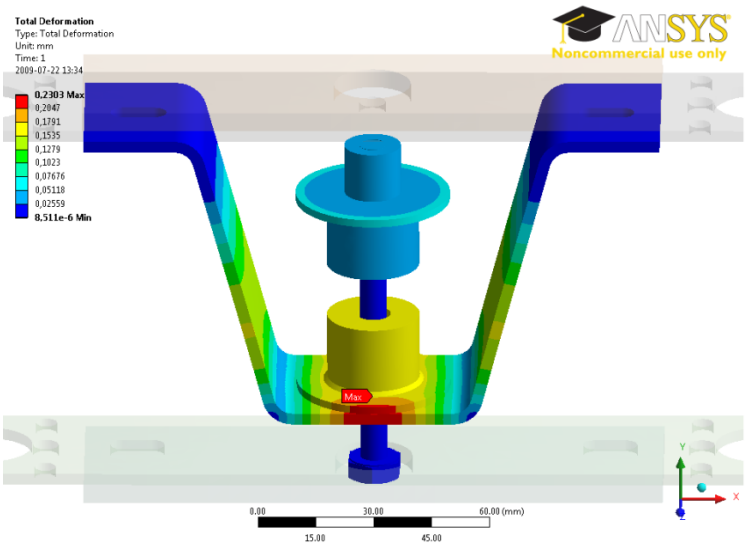

Figure 51. Total deformation.

The maximum equivalent stress of 231 MPa is on the edge of the feather holder, see Figure 52, since it is on the edge it could be a singularity and the result is unreliable. Even thought it is very high it still is within the limits of the material and will be ok in any case.

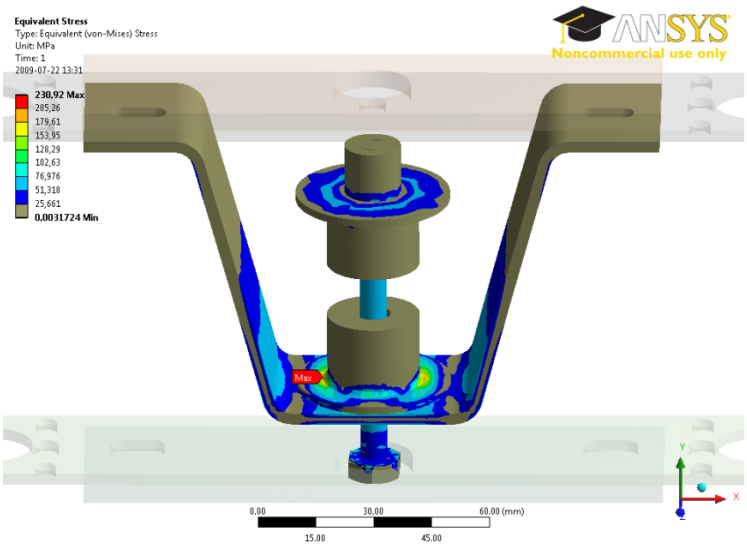

Figure 52. Equivalent stress.

A better close up on the high stress area, in Figure 53, gives a better view of how the stress is affecting the feather holder. The yellow area has a stress in the area of 180 MPa, which give a safety factor of 1.56.

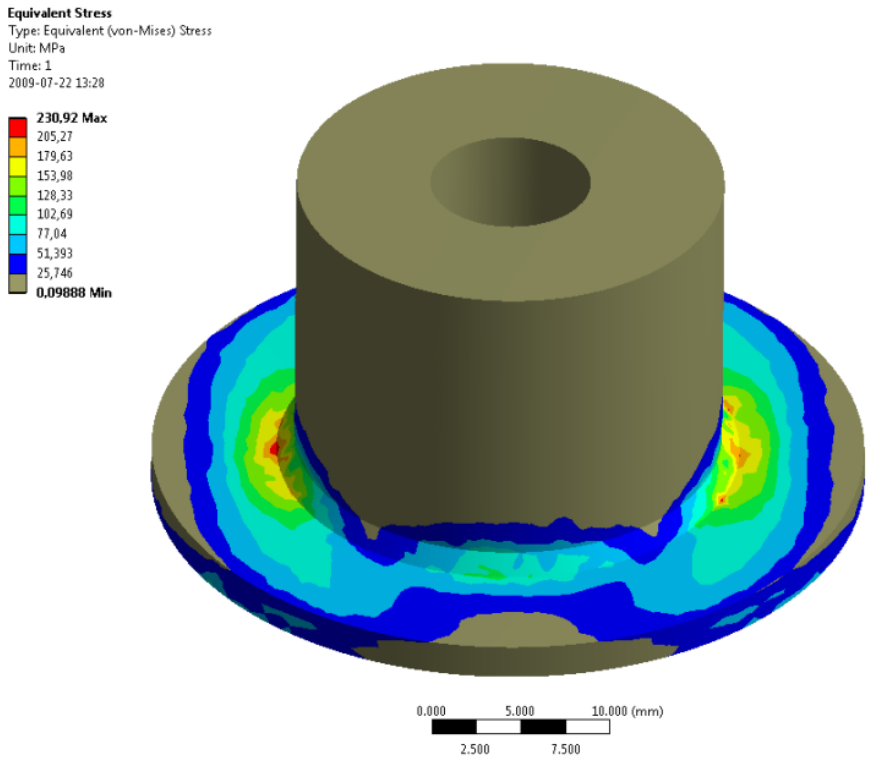

Figure 53. Equivalent stress for feather holder.

5.7 Prototype Finalization

Before building the prototype there are some more components to the whole test rig that have to be finished. One of those is the motor that will propel the test rig, further information about how it was decided upon is written below. An assembly of the fully completed prototype design of the new test rig can be seen in Figure 54

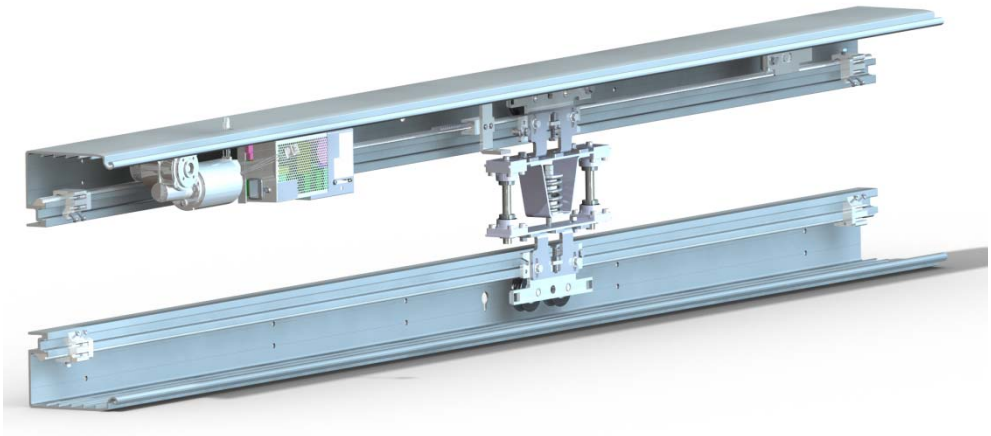

Figure 54. Full test rig assembly.

5.7.1 Test Rig Motor

A reuse of the reference test rig's motion system was used in the design of the first prototype, since as many original parts as possible was used to decrease any unnecessary costs and decrease the delivery time. The reference test rig uses a GR 63x25 50 W DC-motor, but another more powerful motor is available, the GR 63x55 100 W DC-motor. The current GR 63x25 motor has a gearbox mounted on it producing a reduction ratio of 10:1, since our new prototype will weight less then the original it will require less torque to reach the same acceleration and speed. Then it is possible to use the stronger DC-motor and put on a gearbox of 5:1 instead thus increasing the speed and making the test go faster.

- **Given values of the GR 63x25 DC-motor:**
  Continuous rated torque, $M_0 = 133\ mNm$
  Gear efficiency, $E_g = 0.65$
  Gear ratio, $R_g = 10:1$
  Gear wheel diameter, $D_g = 40\ mm$
  No load speed, $n_0 = 3800\ rpm$
  Stall torque, $M_H = 1180\ mNm$
- **Calculations:**
  Continuous torque output with gear, $\tau_g = \left(\frac{\tau_c}{1000}\right) * R_g = 1.33\ Nm$
  Force output, $F_g = \frac{\tau_g}{\left(\frac{\frac{\tau_c}{1000}}{2}\right)*(1-E_g+1)} = 49.3\ N$
  Slope, $S = \frac{n_0}{\frac{M_H}{1000}} = -3220$
  Speed loss, $n_l = \frac{S}{\frac{M_0}{1000}} = -428.3\ rpm$
  Motor speed, $n_M = n_0 + n_l = 3372\ rpm$
  Output speed, $n = \frac{n_M}{R_g} = 337.2\ rpm, v = \left(\frac{n}{60}\right) * 2\pi * \left(\frac{D_g}{2000}\right) = 0.7\ m/s$

Table 10. DC-motor Data.

Motor Data	**GR 63x25, 50 W, 10:1**	**GR 63x55, 100W, 5:1**	
Continuous rated torque	0.133	0.270	Nm
Gear efficiency	65	70	%
Gear ratio	10	5	
Gear wheel diameter	40	40	mm
No load speed	3800	3600	rpm
Stall torque	1.18	2.10	Nm
Calculated Values			
C.R.T. output with gear	1.33	1.35	Nm
Force output	49.3	51.9	N
Slope	-3220	-1714	
Speed loss	-428.3	-462.9	rpm
Motor speed	3372	3137	rpm
Output speed, rpm	337.2	627.4	rpm
Output speed, m/s	0.7	1.3	m/s

5.8 Prototype Design

The prototype was designed at ASSA ABLOY Entrance Systems testing workshop. The currently existing test rigs that are being used by the company can be seen in Figure 55, where a door with a set weight is used.

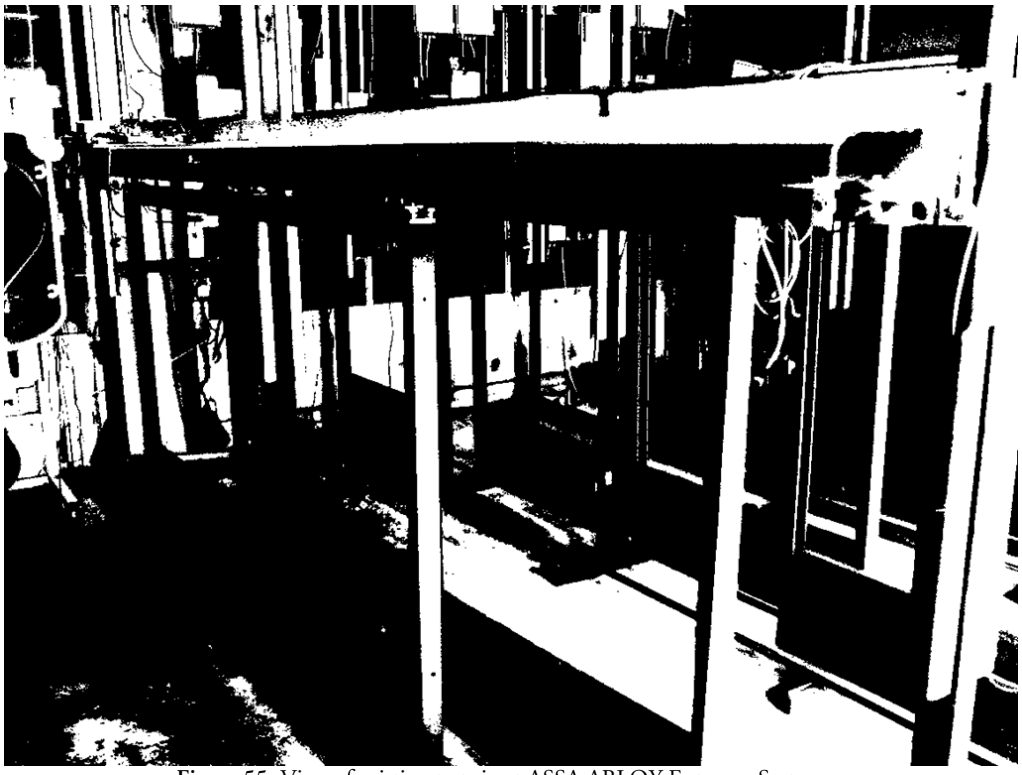

Figure 55. View of existing test rig at ASSA ABLOY Entrance Systems.

All components for the prototype was ready to be assembled, Figure 56, and it took about one and a half-day to complete the prototype. During the process, some small issues like how to mount the aluminium profile upside down had to be solved during the assembly process.

Figure 56. Drawings and parts before the assembly.

The prototype design began with mounting one extra aluminium profile under the present one. The track on the new one was screwed to place since it otherwise would fall down. The sliding wheel design was then mounted and adjusted so it would fit in between the two profiles (see Figure 57).

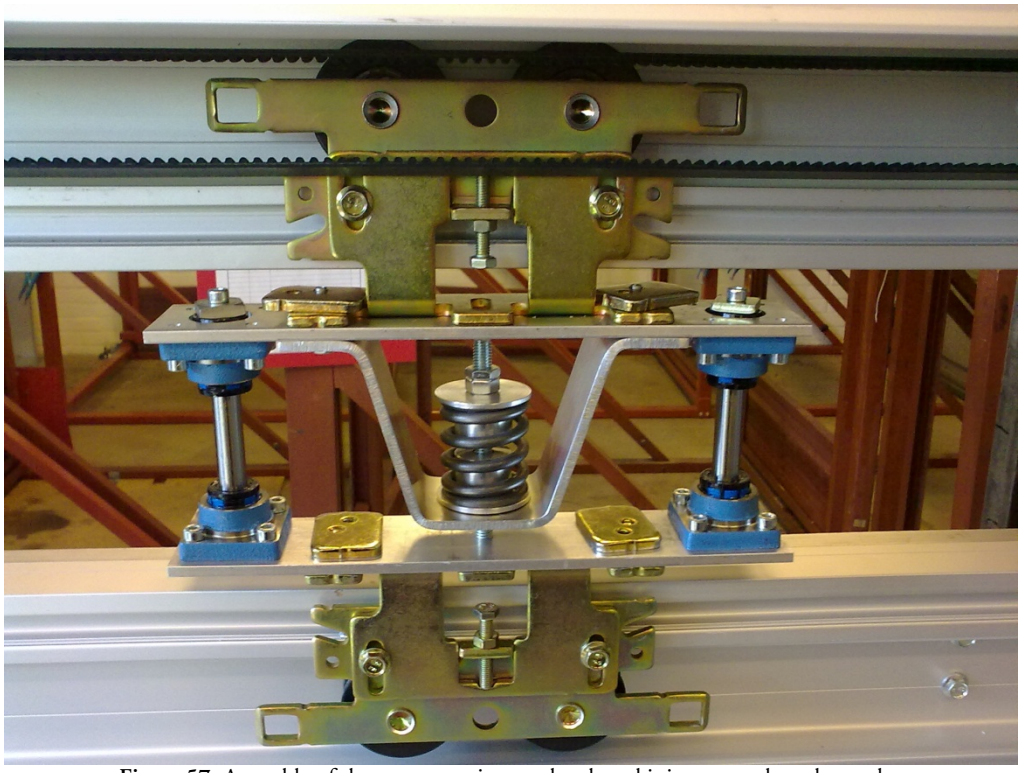

Figure 57. Assembly of the contractor is completed, and it is mounted on the track.

5.9 Prototype Testing

Pretension the spring to so a contact force of about 270 N to each wheel was achieved and tested the sliding door for a few cycles. No extensive testing could be done with the current instalment since the motor had been damaged in an earlier test, not connected to our study. Even though the test was conducted with a damaged motor, the movement of the prototype was fast in relation to the reference test rig.

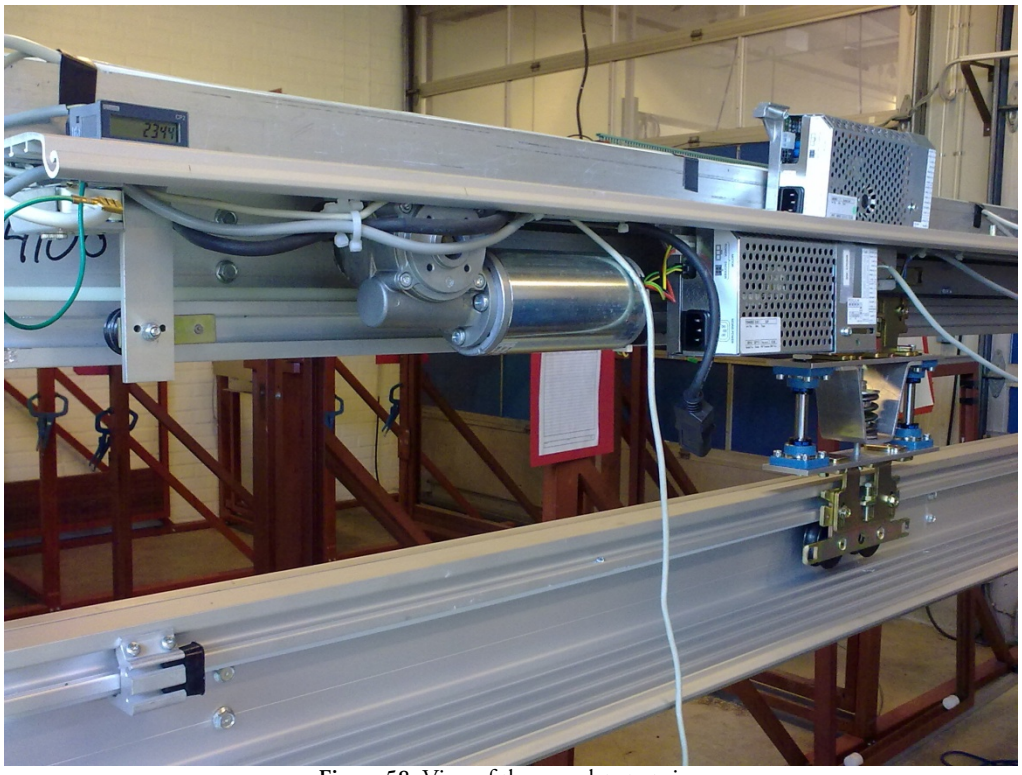

Figure 58. View of the complete test rig.

5.9.1 Cycle Time

To get a result from the Prototype Testing a mathematical analysis where conducted since no practical testing could be done. In the analysis rolling resistance and friction where excluded. As reference a test rig with two 100 kg doors on a 4 m track were used. The doors travel towards each other, which results in a maximum motion distance of 2 m. Top velocity where set to 0.7 m/s, which is the present maximum velocity.

Two prototypes where use in the comparison to get same amount of wheel contacts. The new rig has a mass of less than 2 kg, therefore the new calculated top velocity of 1.3 m/s where used.

- **Calculations:**

  Available Power: $P = \frac{F*s}{t} = 70\ W$

  Newton's second law: $F_{res} = ma$

  Acceleration: $a = \frac{v}{t}$

  Motion distance: $s = t * v_m = t * \frac{v}{2}$

  Time to accelerate a mass (m) to a velocity (v) with Power (P): $t = \frac{m*v^2}{2*P}$

  Total time for one cycle: $t_{cycle} = 2 * (2t_{acc} + t_{const})$

Table 11. Cycle time calculations.

Data	**Present rig**	**Prototype rig**	
Power	70	70	W
Motion distance	2	2	m
Maximum velocity	0.7	1.3	m/s
Mass	200	4	kg
Calculated values			
Acceleration			
Time	0.700	0.048	s
Distance	0.245	0.031	m
Constant velocity			
Distance	1.510	1.937	m
Time	2.157	1.490	s
Total cycle time	7.114	3.173	s

Mathematical analysis results in a decrease of cycle time by 55 percent when the cycle has no pauses. If this relation remains during the entire test, one--million cycle test could take only 2.7 months instead of 6 months. This result only gives guidance what a proper test would result in since friction and rolling resistance were excluded.

5.10 Discussion

Throughout the selection process most decisions was based on economic foundations. As many standard components from ASSA ABLOY Entrance Systems was used to make an eventual transition of this new form of testing rig as easy as possible. Once completed many aspects in its design was more clearly visible and new ideas of improvement came into place. Like for example a possibility to join more contractors together to make it more stable and more similar to an actual door.

A better ability to change the angles of the wheel should also be implemented in a newer version of the prototype so that easier study of what might happen dying an incorrect installation.

Another way of solving how to connect the track to the lower aluminium profile should be developed as well. This problem have been partly solved since the alternative wheels that has plastic layer uses an aluminium track instead and therefore possesses no problem, but if studies using a nylon track could be used in the future this need to be fixed. In the end, not much time was available for a longer test run of the new test rig, this is also recommended to do in a future study.

6. Conclusions

6.1 Theoretical Model

To limit the developing time there was an interest in developing a theoretical model, which could predict the lifetime of a wheel with the help of different input values.

With the mathematical model created in the study, it is possible to predict lifetime of a wheel/track combination by imputing data from a short time test with high contact force. Then it will be able to predict how long a test using normal contact forces will last. In addition, it will be possible to optimize the wheel/track to make them smaller if a specific pressure is given.

6.2 Practical Device

The second aim for the study was to create a different type of test rig that could decrease the testing time, and still produce an accurate result similar to a real situation.

The prototype of the new test rig displays that it is possible to design a lightweight testing rig with the possibility to increase the speed of a wheel/track lifetime testing. The new test rig uses the same carriage wheel and sliding track as present test rig. Moreover, all its components are made with an easy conversion in mind and at minimal cost.

6.3 Recommendations for further studies

- Smudge consistence analysis.
- Verification of contact of a real door.
- Verification of Palmgren's relation.
- Verify the minimal temperature rise.
- Test angle of the wheel to simulate incorrect installation.
- Better way of mounting the lower track upside down.
- Design an automotive brush or cleaning interval to remove smudge from the wheel.

7. References

ASSA ABLOY. (2009). *About Us*. Retrieved May 5, 2009, from Besam: http://www.assaablyes.com

Bayer, R. G. (2004). *Mechanical wear fundamentals and testing* (2., rev. and exp. ed.). New York: Marcel Dekker.

Callister, W. D. (2007). *Materials science and engineering : an introduction* (7. ed.). New York, N.Y.: Wiley.

Dorinson, A. (1985). *Mechanics and chemistry in lubrication.* Amsterdam: Elsevier.

Ertz, M., & Knothe, K. (2002). A comparison of analytical and numerical methods for the calculation of temperatures in wheel/rail contact. *Wear 253* , 498-508.

Hamrock, B. J., Jacobson, B., & Schmid, S. R. (2005). *Fundamentals of machine elements* (2. ed.). Boston: McGraw-Hill.

Jacobson, B., & Vedmar, L. (2006). *Maskinelement Tribologi.* Lund.

Johnson, K. L. (1985). *Contact mechanics.* Cambridge: Cambridge Univ. Press.

MATLAB. (2009). *Support*. Retrieved July 21, 2009, from The Mathworks: http://www.mathworks.com/support/

Seherr-Thoss, H. C., Aucktor, E., & Schmelz, F. (2006). *Universal Joints and Driveshafts [electronic resource] : Analysis, Design, Applications* (2nd ed.). Berlin, Heidelberg: Springer-Verlag Berlin Heidelberg.

Shigley, J. E., Mishke, C. R., & Bydynas, R. G. (2003). *Mechanical engineering design* (7 ed.). Boston: McGraw Hill Higher Education.

Stachowiak, G. W., & Batchelor, A. W. (2005). *Engineering Tribology* (3. ed.). Burlington: Elsevier.

Ulrich, K. T., & Eppinger, S. D. (2008). *Product design and development* (4. ed.). Boston, Mass.: McGraw-Hill/Irwin.

Appendix A Contact calculation

Elliptical contact pressure

To calculate deformation (approach of distance point) and pressure the value of major and minor semi-axes (a and b) needs to be calculated first. This requires calculations of the elliptic integrals of the first and second kind. This can be done in different ways, but in this study one more complex and two simplified equations are used.

Equations

- Hertz, (Jacobson & Vedmar, 2006)
- Simplified 1, (Stachowiak & Batchelor, 2005)
- Simplified 2, (Hamrock, Jacobson, & Schmid, 2005)

Hertz

If the angle, between the two bodies coordinate system, is zero the derived equations for contact pressure where all concave surface radii are negative by definition: (Jacobson & Vedmar, 2006, pp. 125-127)

$$2(A+B) = \frac{1}{R_{x,1}} + \frac{1}{R_{y,1}} + \frac{1}{R_{x,2}} + \frac{1}{R_{y,2}} \tag{6}$$

$$2(B-A) = -\frac{1}{R_{x,1}} + \frac{1}{R_{y,1}} - \frac{1}{R_{x,2}} + \frac{1}{R_{y,2}} \tag{7}$$

$$\begin{aligned} A &= p_{max}(k_1+k_2)\frac{b}{e^2a^2}\left(\mathbf{K}(e) - \mathbf{E}(e)\right) \\ B &= p_{max}(k_1+k_2)\frac{b}{e^2a^2}\left(\frac{a^2}{b^2}\mathbf{E}(e) - \mathbf{K}(e)\right) \\ \delta &= p_{max}(k_1+k_2)b\mathbf{K}(e) \end{aligned} \tag{8}$$

where **E** and **K** are the elliptic integrals of the first and second kind and:

$$k_i = \frac{1 - \nu_i^2}{E_i} \tag{9}$$

$$e = \sqrt{1 - \frac{b^2}{a^2}}, \qquad a > b \tag{10}$$

$$\begin{aligned} \mathbf{K}(e) &= \int_0^{\frac{\pi}{2}} \frac{d\theta}{\sqrt{1 - e^2 \sin^2\theta}} \\ \mathbf{E}(e) &= \int_0^{\frac{\pi}{2}} \sqrt{1 - e^2 \sin^2\theta}\, d\theta \end{aligned} \tag{11}$$

$$F = \frac{B - A}{B + A} \Longrightarrow \frac{B}{A} = \frac{1 + F}{1 - F} \Longrightarrow \frac{B}{A} - \frac{1 + F}{1 - F} = 0 \tag{12}$$

Inserting equation (8), (10) in equation (12) permit a solution for *a*/*b*

$$\frac{\frac{a^2}{b^2}\mathbf{E}\left(\sqrt{1 - \frac{b^2}{a^2}}\right) - \mathbf{K}\left(\sqrt{1 - \frac{b^2}{a^2}}\right)}{\mathbf{K}\left(\sqrt{1 - \frac{b^2}{a^2}}\right) - \mathbf{E}\left(\sqrt{1 - \frac{b^2}{a^2}}\right)} - \frac{1 + F}{1 - F} = 0 \implies \frac{a}{b} \tag{13}$$

Combining this solution for a/b with (4) and (8) give the final equation for major and minor semi-axes and deformation for the contact.

$$\begin{aligned} a &= a_0 \sqrt[3]{\frac{3}{4}\frac{k_1 + k_2}{A + B} P}, \qquad a_0 = \sqrt[3]{\frac{3}{\pi}\frac{\frac{a^2}{b^2} - 1}{1 - \frac{b^2}{a^2}}\mathbf{E}} \\ b &= b_0 \sqrt[3]{\frac{3}{4}\frac{k_1 + k_2}{A + B} P}, \qquad b_0 = a_0 \frac{b}{a} \\ \delta &= \delta_0 \sqrt[3]{\frac{9}{16}(k_1 + k_2)^2 P^2 (A + B)}, \qquad \delta_0 = \frac{2\mathbf{K}}{\pi a_0} \end{aligned} \tag{14}$$

With the value from equation (14), the pressure can be calculated in equation (4).

Simplified equations

Another way to calculate the contact pressure is to use simplified equations. This is quicker way of calculation that gives similar result.

The two simplified equations uses the same basic equations, these are:

$$E = \frac{2}{k_1 + k_2} \tag{15}$$

$$\frac{1}{R_x} = \frac{1}{R_{x,1}} + \frac{1}{R_{x,2}} \tag{16}$$

$$\frac{1}{R_y} = \frac{1}{R_{y,1}} + \frac{1}{R_{y,2}} \tag{17}$$

$$\frac{1}{R} = \frac{1}{R_x} + \frac{1}{R_y} \tag{18}$$

$$a = \sqrt[3]{\frac{6k_e^2 \mathcal{E} P R}{\pi E}}$$

$$b = \sqrt[3]{\frac{6\mathcal{E} P R}{\pi k_e E}} \tag{19}$$

$$\delta = \mathcal{F} * \sqrt[3]{\left(\frac{9}{2\mathcal{E}R}\right)\left(\frac{P}{\pi k_e E}\right)^2}$$

Where $\mathcal{F}$, $\mathcal{E}$ are the elliptic integrals and k_e ellipticity parameter

Simplified 1

Specific equation for Simplified equation according to (Stachowiak & Batchelor, 2005)

$$\mathcal{F} = 1.5227 + 0.6023 \ln\left(\frac{R_y}{R_x}\right) \tag{20}$$

$$\mathcal{E} = 1.0003 + \frac{0.5968 R_x}{R_y} \tag{21}$$

$$k_e = 1.0339 + \left(\frac{R_y}{R_x}\right)^{0.636} \tag{22}$$

Simplified 2

Specific equation for Simplified equation according to (Hamrock, Jacobson, & Schmid, 2005)

$$\alpha_r = \frac{R_y}{R_x} \tag{23}$$

$$k_e = \alpha_r^{\frac{2}{\pi}} \tag{24}$$

$$q_a = \frac{\pi}{2} - 1 \tag{25}$$

Calculating the elliptic integrals depend on the size of radii ratio α_r

$$1 \leq \alpha_r \leq 100, \qquad 0.01 \leq \alpha_r \leq 1.0 \tag{26}$$

$$\mathcal{F} = \frac{\pi}{2} + q_a \ln \alpha_r\,, \qquad \mathcal{F} = \frac{\pi}{2} - q_a \ln \alpha_r \tag{27}$$

$$\mathcal{E} = 1 + \frac{q_a}{\alpha_r}, \qquad \mathcal{E} = 1 + q_a \alpha_r \tag{28}$$

Principal stresses and maximum shear stress

If major and minor semi axis of contact is about the same, methods to calculate the principal stresses and maximum sheer stress calculates as below (Shigley, Mishke, & Bydynas, 2003, pp. 162-163). The method to calculate stress for all point contact types were not used in this study due to its complexity.

For circular contact, stresses in x and y direction become the same. This gives the first principal stress as:

$$\sigma_1 = \sigma_x = -p_{max}\left[\left[1 - |\zeta_a| \tan^{-1}\left(\frac{1}{|\zeta_a|}\right)\right](1+\nu) - \frac{1}{2(1+\zeta_a^2)}\right] \tag{29}$$

$$\sigma_3 = \sigma_z = \frac{-p_{max}}{(1+\zeta_a^2)} \tag{30}$$

$$\zeta_a = \frac{z}{a} \tag{31}$$

Where z is distance from surface and ν Poisson's ratio of calculated material.

The definition of maximum shear stress according to Mohr's circle of stress becomes

$$\tau_{max} = \frac{\sigma_1 - \sigma_3}{2} \tag{32}$$

Appendix B Microscopic Images

Steel Wheel

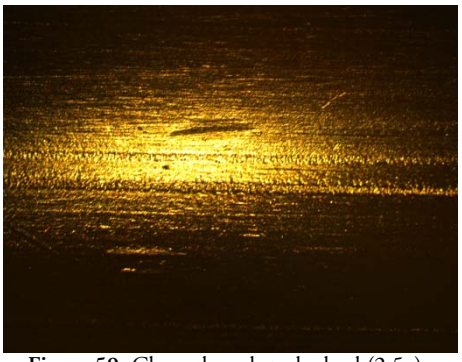

Figure 59. Cleaned used steel wheel (2.5x).

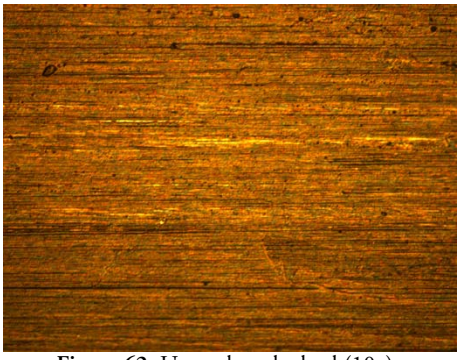

Figure 62. Unused steel wheel (10x).

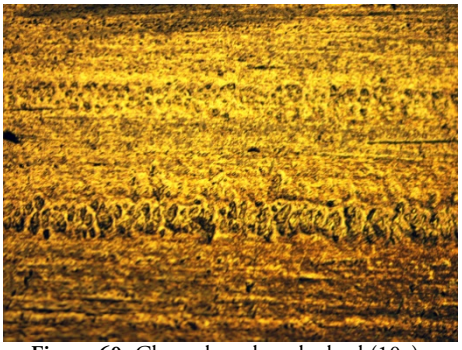

Figure 60. Cleaned used steel wheel (10x).

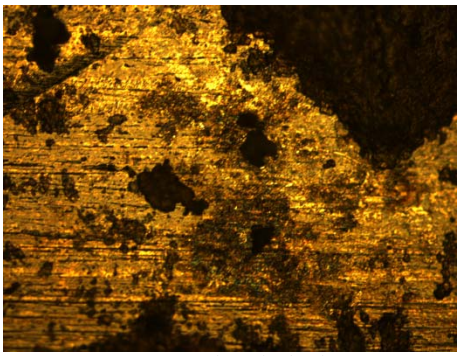

Figure 63. Used steel wheel (10x).

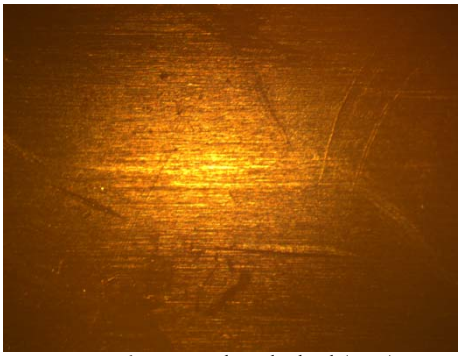

Figure 61. Unused steel wheel (2.5x).

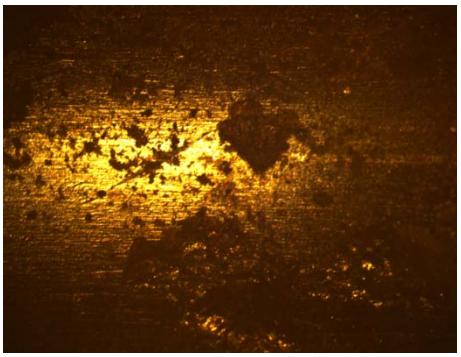

Figure 64. Used steel wheel (2.5x).

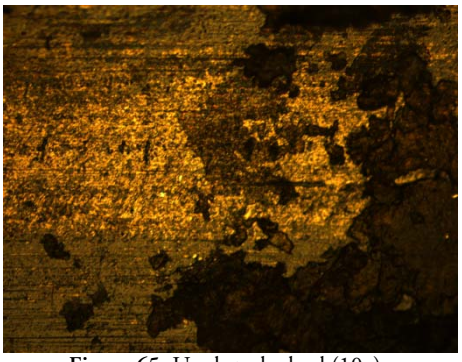

Figure 65. Used steel wheel (10x).

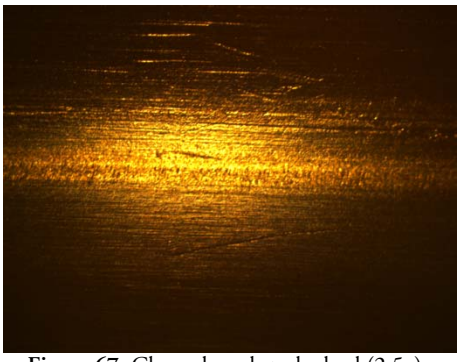

Figure 67. Cleaned used steel wheel (2.5x).

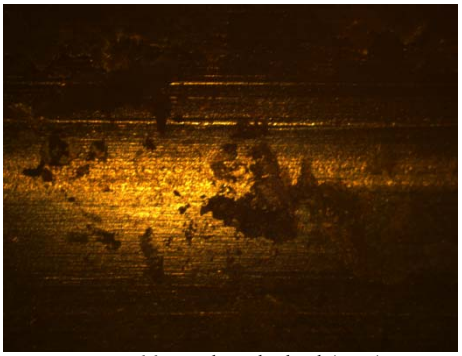

Figure 66. Used steel wheel (2.5x).

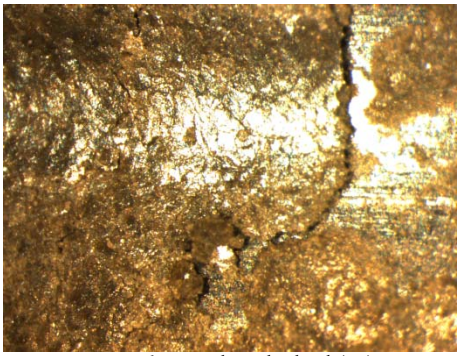

Figure 68. Used steel wheel (8x).

Plastic Wheel

Figure 69. Used plastic wheel (10x).

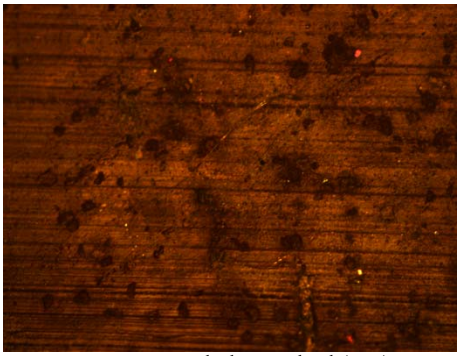

Figure 72. Used plastic wheel (10x).

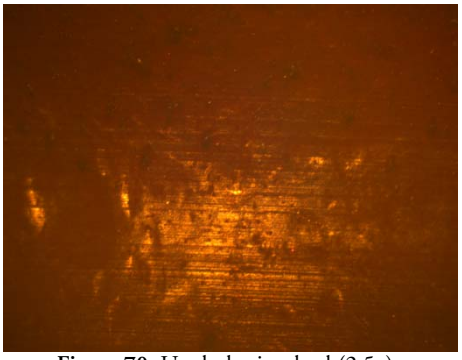

Figure 70. Used plastic wheel (2.5x).

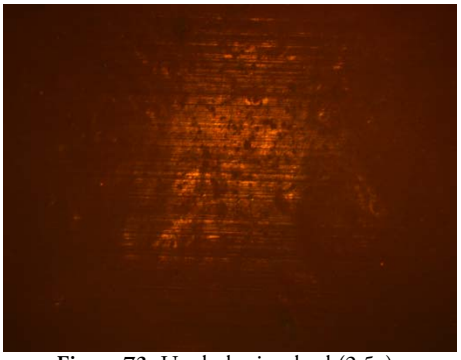

Figure 73. Used plastic wheel (2.5x).

Figure 71. Unused plastic wheel (10x).

Nylon Track

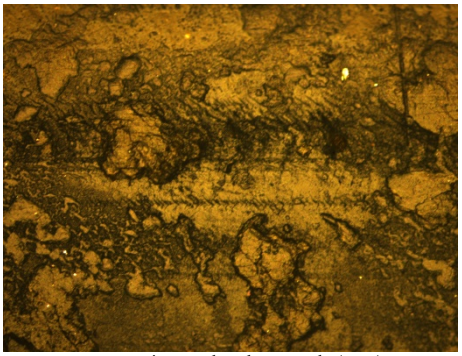

Figure 74. Used nylon track (10x).

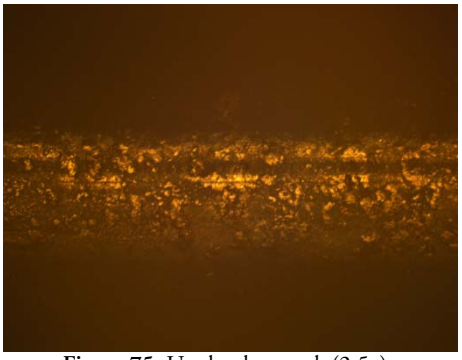

Figure 75. Used nylon track (2.5x).

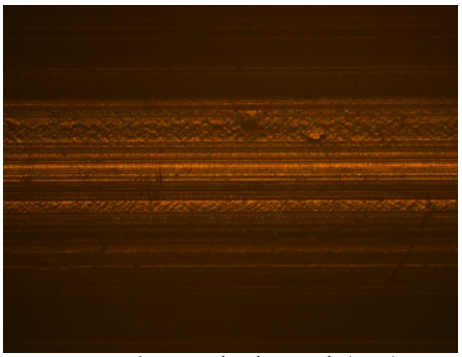

Figure 76. Unused nylon track (2.5x).

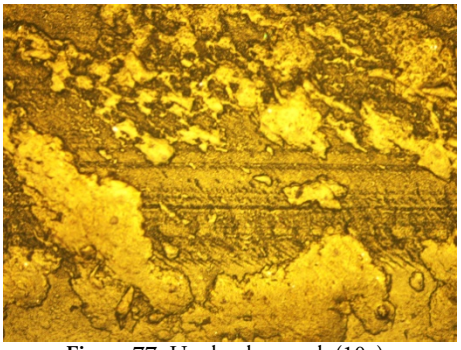

Figure 77. Used nylon track (10x).

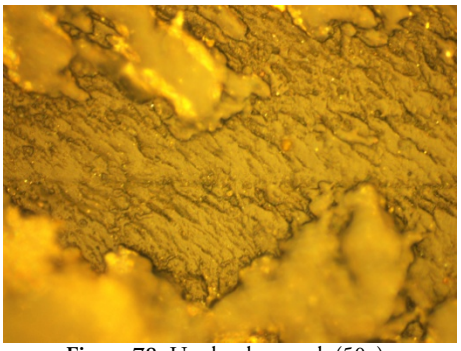

Figure 78. Used nylon track (50x).

Appendix C Wheel optimization data

Table 12. Free combinations.

Force	Pressure (Pa)	a (m)	b (m)	Rx1 (m)	Ry1 (m)	Ry2 (m)	Ry1/Ry2
500N	75866733	0.0021515	0.0014626	0.0210	-0.0075	0.00625	-1.200
450N	76748663	0.0021164	0.0013228	0.0185	-0.0075	0.00625	-1.200
400N (1)	76162789	0.0020598	0.0012174	0.0170	-0.0075	0.00625	-1.200
400N (2)	76681407	0.0021336	0.0011674	0.0160	-0.0085	0.00700	-1.214
350N (1)	75436483	0.0019960	0.0011098	0.0155	-0.0075	0.00625	-1.200
350N (2)	75179385	0.0020589	0.0010796	0.0150	-0.0085	0.00700	-1.214
300N (1)	72559511	0.0019047	0.0010364	0.0150	-0.0075	0.00625	-1.200
300N (2)	74211701	0.0018352	0.0010517	0.0150	-0.0080	0.00650	-1.231
250N	72848862	0.0016120	0.0010165	0.0150	-0.0075	0.00600	-1.250

Table 13. Fix Ry1, Ry2 combinations.

Force	Pressure (Pa)	a (m)	b (m)	Rx1 (m)	Ry1 (m)	Ry2 (m)	Ry1/Ry2
org 500N	75708541	0.0020533	0.0015357	0.0225	-0.00725	0.006	-1.208
500N	78992040	0.0020904	0.0014458	0.0200	-0.00725	0.006	-1.208
450N	76972573	0.0020259	0.0013778	0.0195	-0.00725	0.006	-1.208
400N	77013732	0.0019793	0.0012529	0.0175	-0.00725	0.006	-1.208
350N	75291369	0.0019094	0.0011624	0.0165	-0.00725	0.006	-1.208
300N	74129579	0.0018386	0.0010510	0.0150	-0.00725	0.006	-1.208
250N	69758605*	0.0017301	0.0009890	0.0150	-0.00725	0.006	-1.208

* Pressure below 5% limit

Free radii

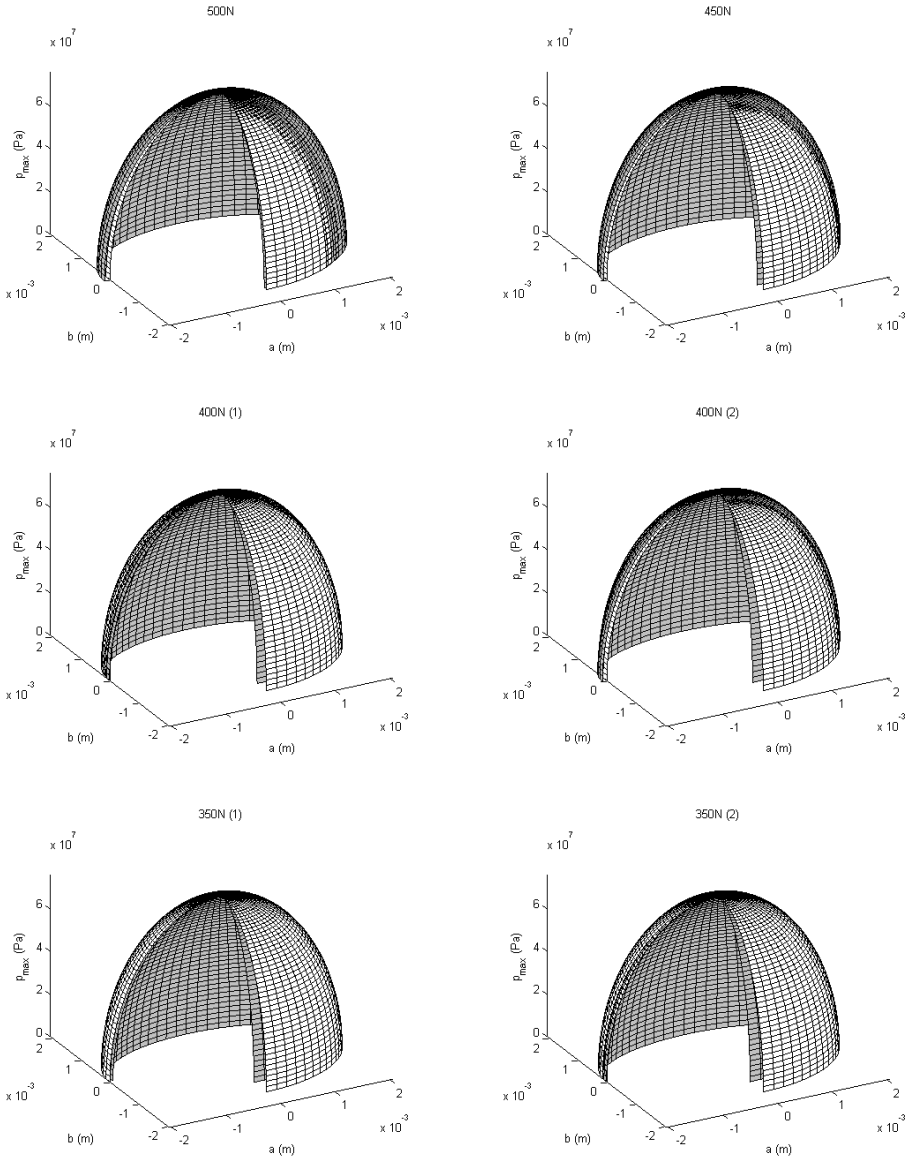

Figure 79. Illustration of contact pressure for the free radii combinations.

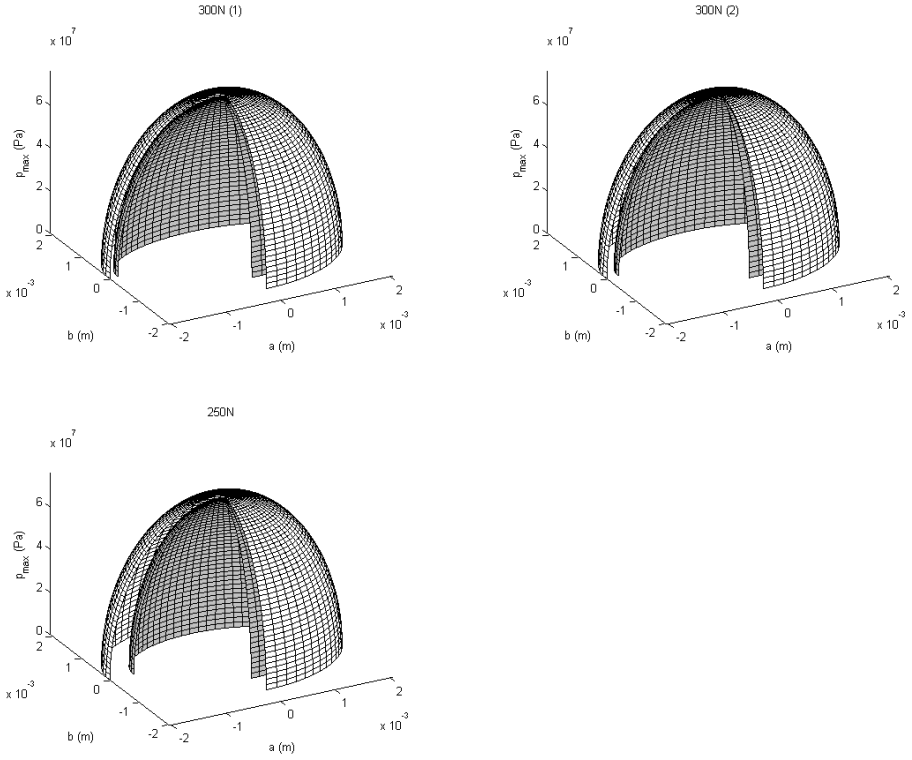

Figure 80. Illustration of contact pressure for the free radii combinations.

Fixed radii

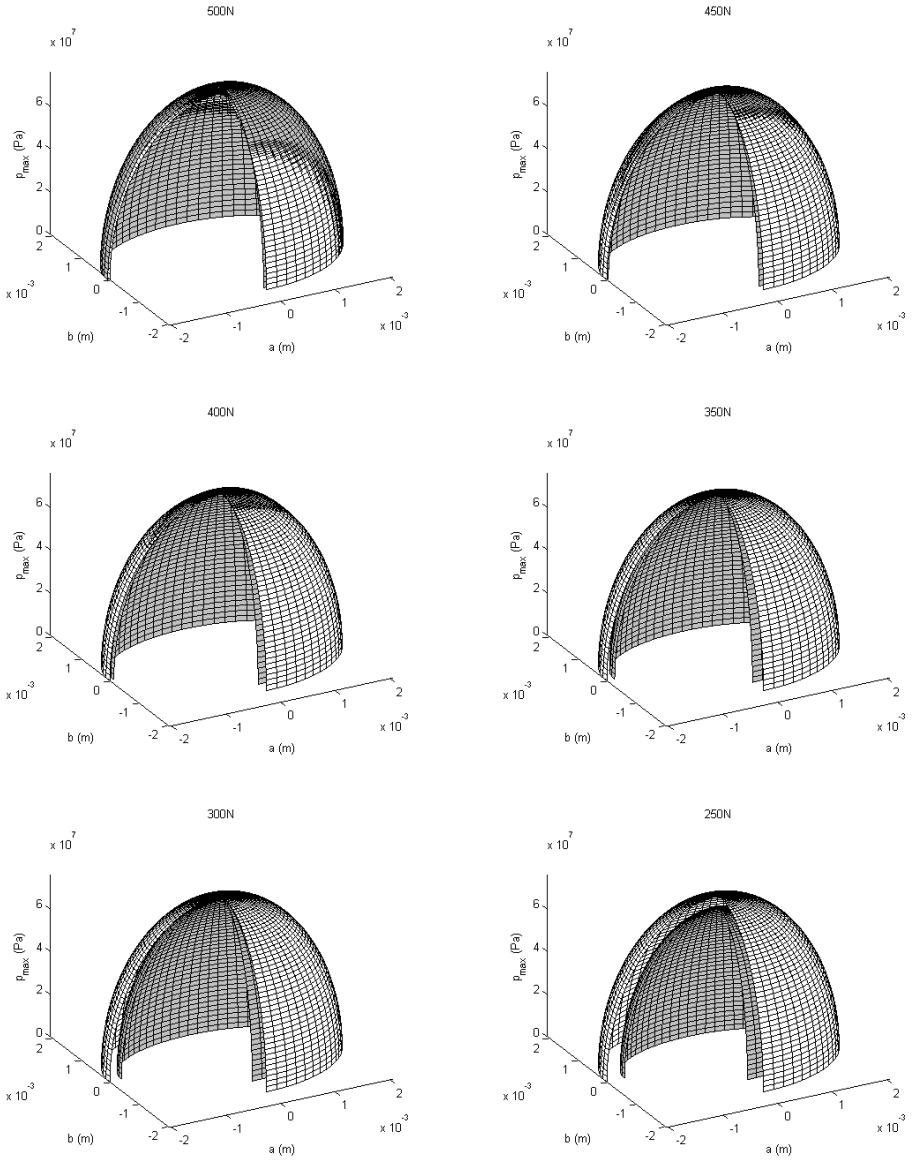

Figure 81. Illustration of contact pressure for the fixed combinations.

Appendix D Drawings

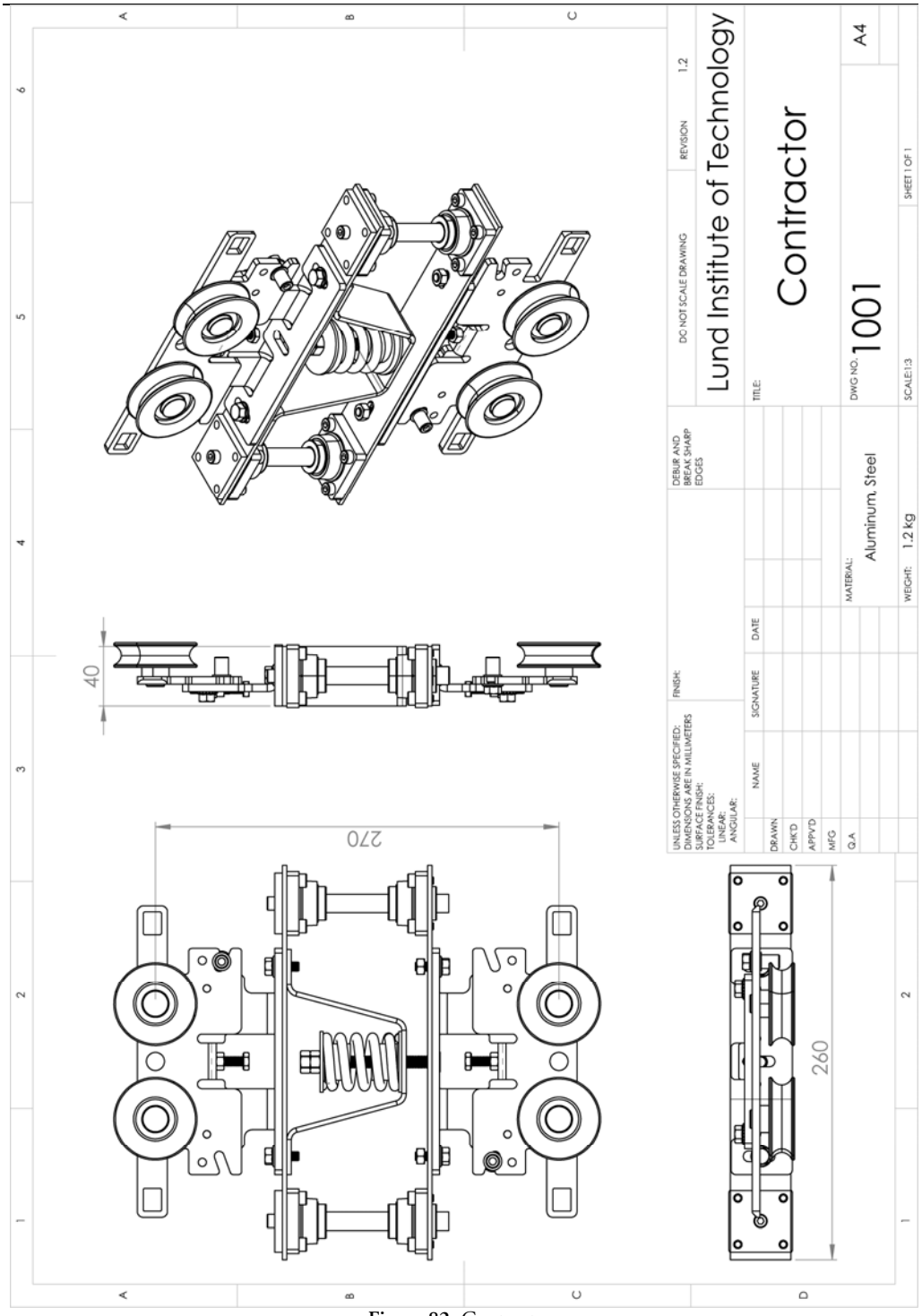

Figure 82. Contractor

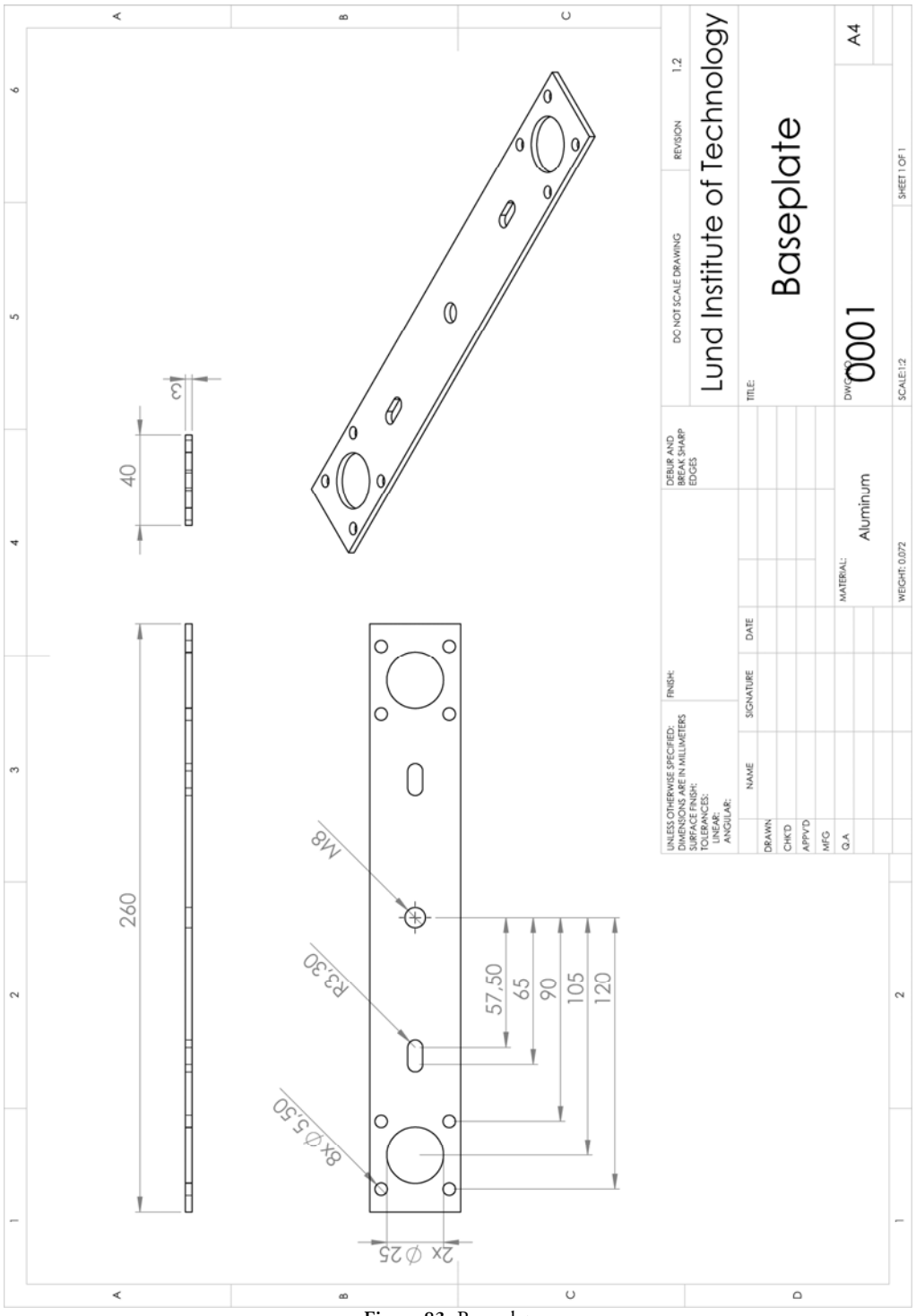

Figure 83. Base plate.

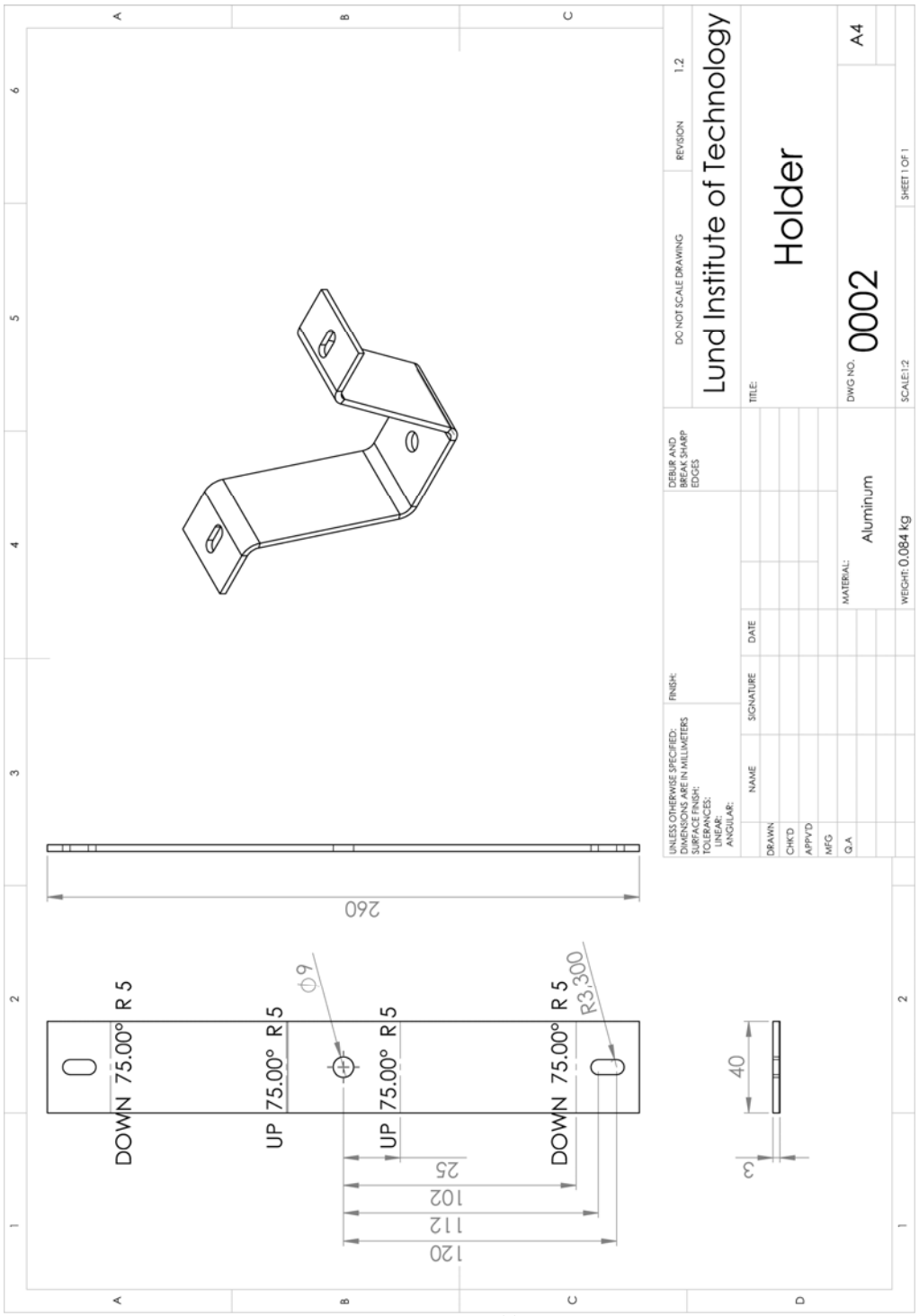

Figure 84. Holder

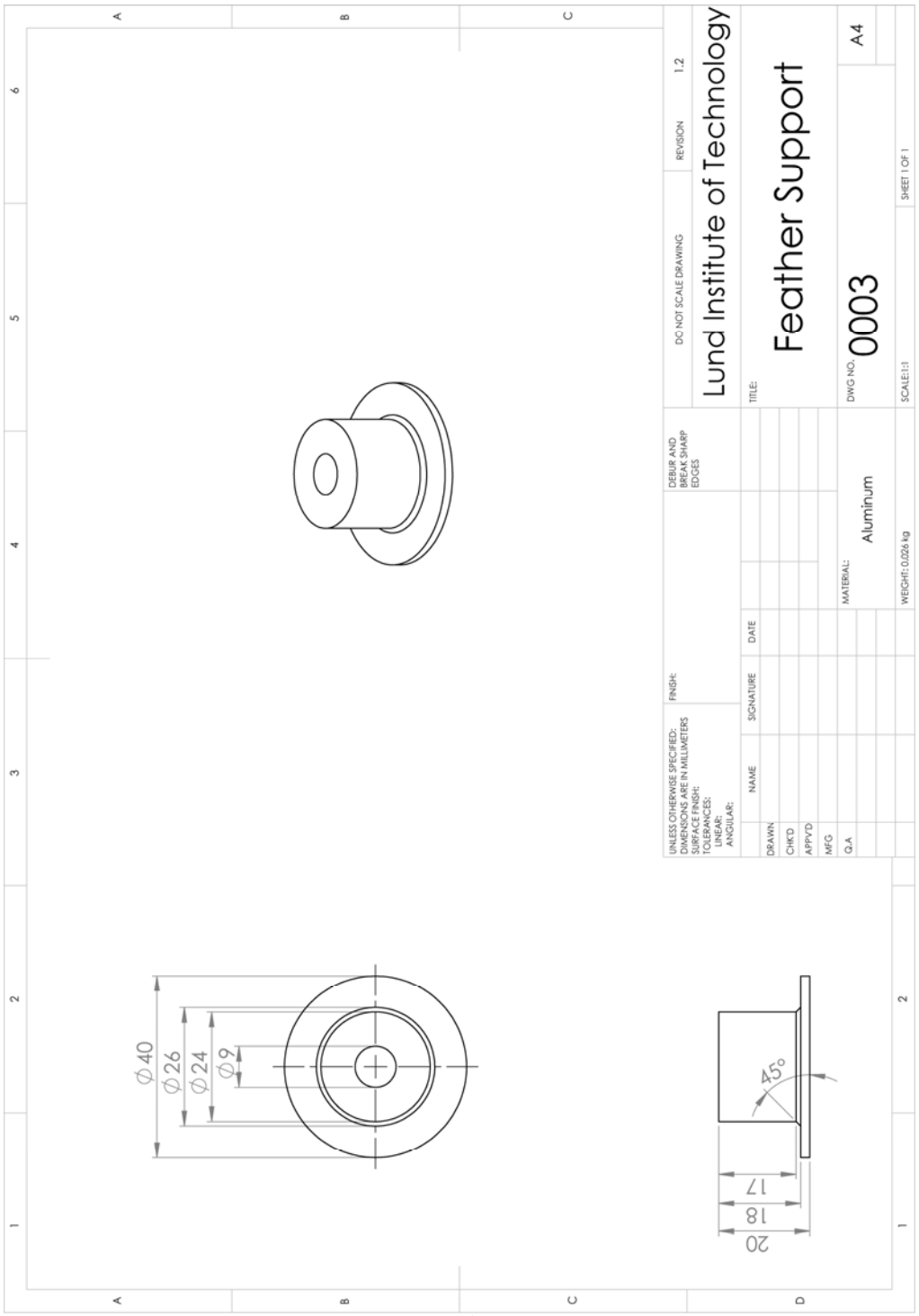

Figure 85. Feather support.

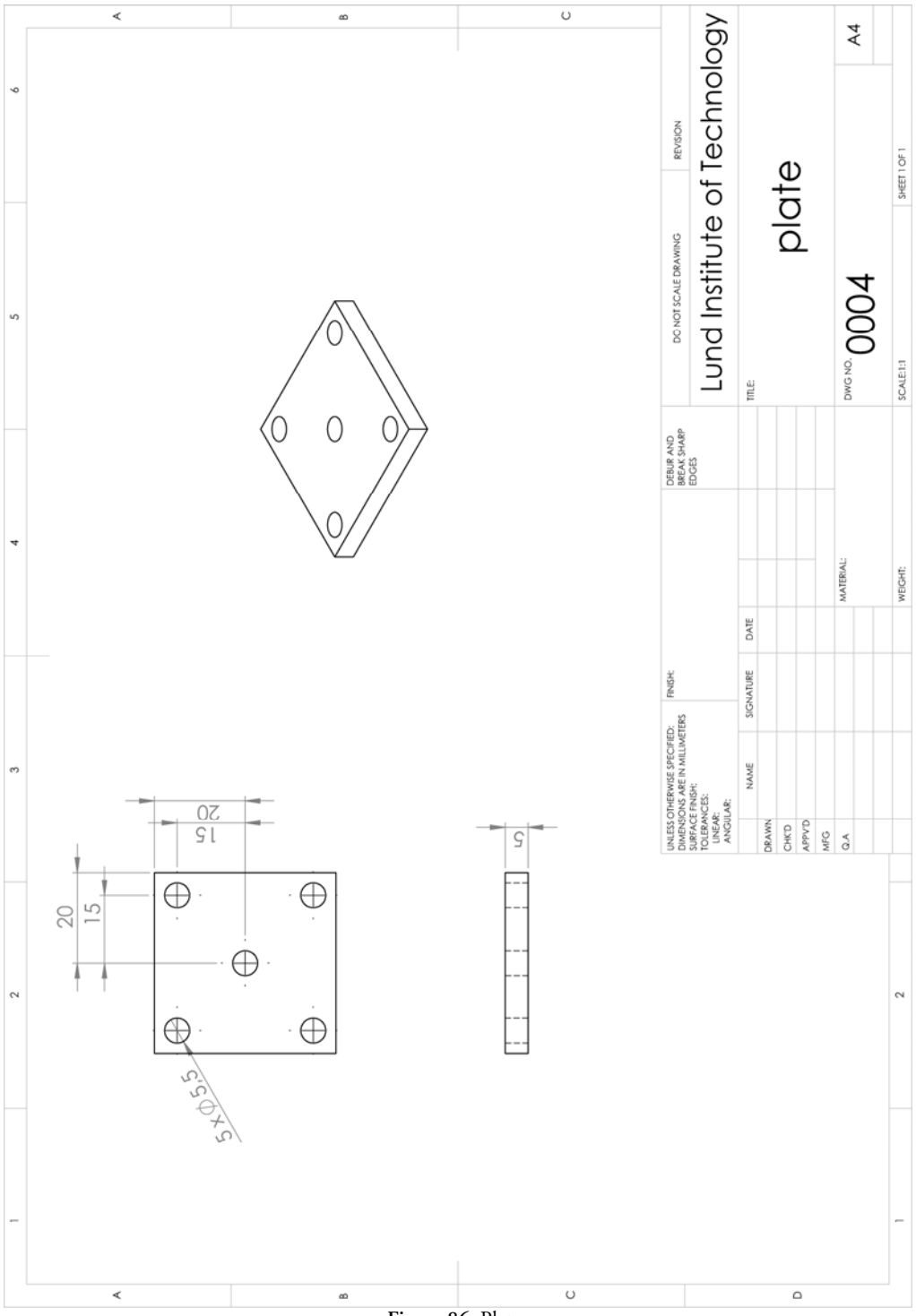

Figure 86. Plate